Sub-micron particle number size distribution characteristics at two urban locations in Leicester

Sarkawt M.L. Hama [1] [2], Rebecca L. Cordell [1], Gerard P.A. Kos [3], E.P. Weijers [3] and Paul S. Monks [1]

[1] Department of Chemistry, University of Leicester, Leicester LE1 7RH, UK
[2] Department of Chemistry, School of Science, University of Sulaimani, Sulaimani, Iraq
[3] Energy research Centre of the Netherlands (ECN), Environment & Energy Engineering, The Netherlands

Correspondence to: Paul S. Monks (psm7@le.ac.uk)

Highlights

- Total particle number concentrations were dominated by nucleation and Aitken modes.
- School holiday has impact on particle number size distribution (PNSD) during Easter.
- The frequency of new particle formation events (NPF) was higher than previous studies in the urban UK.

Keywords: Particle size distribution, Easter holiday, Temporal variation, New particle formation

Abstract

The particle number size distribution (PNSD) of atmospheric particles not only provides information about sources and atmospheric processing of particles, but also plays an important role in determining regional lung dose. Owing to the importance of PNSD in understanding particulate pollution two short-term campaigns (March-June 2014) measurements of sub-micron PNSD were conducted at two urban background locations in Leicester, UK. At the first site, Leicester Automatic Urban Rural Network (AURN), the mean number concentrations of nucleation, Aitken, accumulation modes , the total particles, equivalent black carbon (eBC) mass concentrations were 2002, 3258 , 1576 , 6837 # cm^{-3}, 1.7 μg m^{-3}, respectively, and at the second site, Brookfield (BF), were 1455, 2407, 874, 4737 # cm^{-3}, 0.77 μg m^{-3}, respectively. The total particle number was dominated by the nucleation and Aitken modes, with both consisting of 77%, and 81% of total number concentrations at AURN and BF sites, respectively. This behaviour could be attributed to primary emissions (traffic) of ultrafine particles and the temporal evolution of mixing layer. The size distribution at the AURN site shows bimodal distribution at ~22 nm with a minor peak at ~70 nm. The size distribution at BF site, however, exhibits unimodal distribution at ~35 nm. This study has for the first time investigated the effect of Easter holiday on PNSD in UK. The temporal variation of PNSD demonstrated a good degree of correlation with traffic-related pollutants (NO_X, and eBC at both sites). The meteorological conditions, also had an impact on the PNSD and eBC at both sites**.** During the measurement period, the frequency of NPF events was calculated to be 13.3%, and 22.2% at AURN and BF sites, respectively. The average value of formation and growth rates of nucleation mode particles were 1.3, and 1.17 cm^{-3} s^{-1} and 7.42, and 5.3 nm h^{-1} at AURN, and BF sites, respectively. It can suggested that aerosol particles in Leicester originate mainly from traffic and domestic heating emissions.

1. Introduction

Atmospheric aerosol particles are ubiquitous and have negative impacts on human health, air quality and global climate change (Lohmann and Feichter, 2005; Pope and Dockery, 2006; Stevens and Feingold, 2009). Epidemiological studies have revealed that the existence of a relationship between fine particle concentration and respiratory and cardiovascular diseases (Pope, 2000). Numerous studies have since proposed that ultrafine particles (UFP – particles <100 nm) are more toxic compared to larger particles of same composition and the adverse health effects caused by UFP number concentrations have been indicated to be stronger than those by the fine particle mass concentrations (Peters et al., 1997; Penttinen et al., 2001; Li et al., 2002; Nel, 2005). Nevertheless, current air quality standards are based on the particle mass concentrations. The mass concentrations of the particles less than 100 nm, which really govern the total particle number concentrations in urban areas are insignificant (Seinfeld and Pandis, 1998). Thus, current air quality measurements might be insufficient to permit assumptions to be drawn concerning the association between particle number and the detrimental health effects. It is, therefore, vital to measure the particle number size distributions in order to fully understand the environmental effects of atmospheric ultrafine particles (Peters et al., 1997; Penttinen et al., 2001). Air quality at many urban background sites is influenced by road traffic emissions with diurnal patterns found to be strongly influenced by the primary traffic exhaust emissions in the urban areas (Tuch et al., 2003; Wehner and Wiedensohler, 2003; Hussein et al., 2004; Stanier et al., 2004; Rodríguez and Cuevas, 2007; Pérez et al., 2010). Traffic emissions are considered to be one of the most significant sources of UFP number concentrations in the urban atmosphere, with the other significant source originating from are particile formation (NPF) (Shi et al., 2001; Stanier et al., 2004; Brines et al., 2015). In addition, NPF events can occcur widely under various meteorological and atmospheric conditions (Kulmala et al., 2004; Dal Maso et al., 2005). NPF can be a second source of UFPs in urban areas (Brines et al., 2015). Several NPF studies in rural and urban areas have revealed that NPF is generally favoured under high insolation and wind speed, low relative humidity, and low pre-existing particle surface area (Kulmala et al., 2004; Kulmala and Kerminen, 2008). As such, the increased background concentration of UFPs in polluted areas seems to decrease the NPF. Nevertheless, NPF events are still observed in many polluted urban areas and some of the studies have revealed that strong correlation between the NPF and the levels of vapour-phase H_2SO_4 which is mainly produced by the chemical oxidation of SO_2 with the hydroxyl radical during daytime (Jeong et al., 2004; Kulmala et al., 2012; Zhu et al., 2013; Wang et al., 2014).

eBC is typically formed by incomplete combustion of fossil fuels, biofuel and biomass, and is emitted from traffic. Several studies have shown that a strong relationship between black carbon and road traffic emissions (Fruin et al., 2008; Pérez et al., 2010; Boogaard et al., 2011; Invernizzi et al., 2011; Reche et al., 2011; Butterfield et al., 2015) and biomass burning emissions (Ingrid Sundvor, 2012; Butterfield et al., 2015). Moreover, numerous studies have revealed that exposure to road traffic emissions is best assessed by combining measurements of particle number and eBC concentrations (Harrison et al., 2004; Smargiassi et al., 2005; Rodríguez and Cuevas, 2007), since these parameters need to be controlled by air quality limit values.

In spite of its importance, aerosol size distributions at urban and road sites in UK have been reported at relatively few sites (see Table 1). To our knowledge, there are no studies regarding particle number size distribution measurements and analysis of NPF events in detail in a UK urban area such as Leicester. Information on the behaviour of particle number size distributions is still sparse. There is also a lack of knowledge about particle number size distributions generally in the UK. The objective of the present study is to characterize the NPF events and its impact on PNSD by taking measurements at two sites within the urban area of Leicester. This study also investigates the effect of Easter school holiday on PNSD. Daily and weekly variations of PNSD, and the difference between daily patterns of weekday and weekends of PNSD are explored. The influence of traffic emissions and metrological conditions on PNSD are also investigated.

The study was carried out between March 2014 and June 2014 over which time particle number size distributions (PNSD) were measured concurrently with black carbon mass concentration (eBC), total particle number (TNC), and NO_X at two sites in Leicester. This study reports on the first results of PNSD measurements which were taken as part of the air quality monitoring network established across North West Europe as part of the JOint Air QUality INitiative (JOAQUIN, www.joaquin.eu), an INTERREG IVB funded European project, which aims at supporting health-oriented air quality policies in North-West Europe. More information can be found in the Joaquin report and publications (Joaquin, 2015; Cordell et al., 2016; Hofman et al., 2016; Hama et al., 2017).

2. Experimental

2.1 Sampling sites

The measurements were a part of the JOAQUIN project (www.joaquin.eu). Sampling was conducted during the spring (March-June 2014) at two sites located at the University of Leicester (Figure 1). More detailing about the characteristics and locations of the sampling sites can be found in Hama et al. (2017). In this study hourly traffic density data was provided by Leicester City Council was used. For a detailed overview of the monitoring sites and the JOAQUIN project, the reader is referred to the final report (Joaquin, 2015).

2.2 Instrumentation

Table 2 summarizes the availability of monitors for PNSD, eBC, TNC, NOx and O_3 per site. Measurements at the AURN and BF sites were carried out with the devices in the mobile measurement trailer.

In this study the particle size distribution was measured by a Scanning Mobility Particle Spectrometer (Grimm SMPS+C 5420 with L-DMA). TNC was measured with a TSI model 3783 water-based condensation Particle counter (CPC). This instrument measures the number of particles in the size range of ~7 to 1000 nm. To measure the eBC (Petzold et al., 2013) mass concentration a MAAP (model 5012, Thermo-Scientific) was used. NO_X were measured by a Thermo 42i NO-NO_2-NO_x monitor. The concentrations of O_3 were measured by UV absorption at AURN site. The reference method for the determination of concentrations of O_3 are described in European Standard EN14625, more information can be found in this website (https://uk-air.defra.gov.uk/networks/monitoring-methods?view=eu-standards). For a detailed overview of the instruments and monitors that were used in this study and also about data quality assurance in the JOAQUIN project, the reader is referred to Hama et al. (2017).

Meteorological data were obtained from a mobile laboratory van during this study. Moreover, Meteorological data were also provided by the Air Quality Group from the Leicester City Council, located 4.9 km northwest the AURN site. The mean, median, and max values of wind speed (WS), wind direction (WD), temperature (T), and the relative humidity (RH) form March to May 2014 at both sites are shown in Table 3.

2.3 Data processing and analysis

Particle number concentrations for different size ranges were calculated by the particle size distribution from the Grimm SMPS measurement. The particle number concentrations were categorised into $10 \leq d \leq 1093$ nm (N_{total}), $100 \leq d \leq 1093$ nm (N_{acu}), $25 \leq d < 100$ nm (N_{Aitken}) and $d < 25$ nm (N_{nuc}), for total, accumulation mode, Aitken mode and nucleation mode, respectively. Data analyses have been carried out using the Openair software package (Carslaw and Ropkins, 2012; Carslaw, 2015) using R software (R Core Team, 2014) and sometimes Igor software. The Openair is freely available as an R package.

All data were screened for irregularities. Continuous air quality data collected during instrument errors or maintenance were removed from the analysis. For PNSD, particle losses to the surface of the sampling system and the measuring device can occur via diffusion. Therefore, sampling pipes were kept as short as possible and laminar flow conditions used. Nevertheless, meaningful diffusional losses during sampling and measurement occur for particles <100 μm, so that diffusion correction factors should be applied. For the results of the Grimm SMPS, the diffusion correction factors used were manufacturer factors integrated into the instruments algorithms, after which an additional correction was done using factors based on the simplified expression formula for cylindrical pipes (Hinds, 1999). No other instrument corrections were applied, more detail can be found in the final JOAQUIN report (Joaquin, 2015).

2.4 New particle formation event characteristics

The particle formation rate (J) is defined as the flux of the nucleated particles into the observed nucleation mode particle size range (for example, 10-25 nm , in this study) (Kulmala et al., 2004). The experiential particle formation rate was found by simplified calculation of the general dynamic equation (GDE), describing the evolution of particle size distribution (Seinfeld and Pandis, 2006). The nucleation rate formation ($J_{10\text{-}25}$) was calculated according to Dal Maso et al. (2005), as follows:

$$J_{10-25} = \frac{dN_{10-25}}{dt} + F_{coag} + F_{growth} \qquad (1)$$

where F_{coag} is the flux due to coagulation losses, and F_{growth} is the flux of particles growing out of the nucleation mode size range. $dN_{10\text{-}25}/dt$ is the rate of change of nucleation mode particles with time, t. It should be noted that particles grew out of the freshly nucleated size range of 10-25 nm, as a result F_{growth} term in Eq. (1) cannot be neglected and was calculated by Dal Maso et al. (2005) method as follow:

$$F_{growth} = \frac{1}{\Delta D_p} . GR_{10-25} . N_{10-25} \qquad (2)$$

where, $\Delta Dp = (25\text{-}10) = 15nm$

Here, $GR_{10\text{-}25}$ was obtained from the SMPS data in the size range 10-25 nm, and $N_{10\text{-}25}$ is the number concentration of nucleation mode particles. The coagulation loss for the size range 10-25, F_{coag}, was calculated as:

$$F_{coag} = N_{10-25} . \sum_j K_{ij} . N_j \qquad (3)$$

where $\Sigma K_{ij}.N_j$ is the coagulation sink. N_j is the particle number concentration of size bin j. K_{ij} is the coagulation coefficient between size bin i and j, and is given as (Seinfeld and Pandis, 2006):

$$K_{ij} = 2\pi . (d_i + d_j) . (D_i + D_j) . \beta_{F_{ij}} \qquad (4)$$

where d is the diameter of a size bin, D and β_F are the size dependent diffusion coefficient and Fuchs correction factor of particles, respectively (Seinfeld and Pandis, 2006).

The growth rate (GR) of NPF events is defined as the rate of change in the diameter. The GR was calculated according to Kulmala et al. (2012):

$$GR = \frac{\Delta D_p}{dt} = \frac{Dp_2 - Dp_1}{t_2 - t_1} \qquad (5)$$

where d_{p1} and d_{p2} are the geometric mean diameter of nuclei mode particles and dt is the time interval. The units of GR are nm h^{-1}.

The condensation sink (CS) is a measure of how rapidly vapour molecules will condense onto pre-existing particles and depends mainly on the shape of particle size distribution (Kulmala et al., 2001; Dal Maso et al., 2002; Lehtinen et al., 2003).

An expression for the CS, with unit of s^{-1}, the CS can be calculated as follows (Kulmala et al., 2001):

$$CS = 2\pi . D. \sum_i \beta_{Mi} . d_{pi} . N_i \qquad (6)$$

$$\beta_M = \frac{1 + K_n}{1 + 0.337\, K_n + \frac{4K_n}{3\alpha} + \frac{4K_n^2}{3\alpha}} \qquad (7)$$

where D is the diffusion coefficient for H_2SO_4 (0.104 cm^2 s^{-1}), β_M is the size-dependent transition correction factor, dpi is the aerosol particle diameter, Ni is the particle number concentration, α is mass accommodation coefficient (α=1), and Kn is the Knudsen number can

be expressed in terms of particle diameter and the mean free path vapor molecules (λv) as (Pirjola et al., 1999):

$$K_n = \frac{2\lambda_v}{dp} \qquad (8)$$

The pressure and temperature dependant mean free path of vapour molecule (λv) can be calculated by the following equation from Willeke (1976):

$$\lambda_v = \lambda_r . \left(\frac{101}{P}\right) . \left(\frac{T}{293}\right) . \left(\frac{1 + 110/293}{1 + 110/T}\right) \qquad (9)$$

where P is in kPa and T in K. at 293 K and 1 kPa atmospheric pressure, the λr (mean free path) is 0.039 μm for H_2SO_4. By using this reference value of λr, λv can be calculated for measured pressures and temperatures during NPF event days at the sampling sites. By using these above equations and measured PNSD at AURN and BF sites, the CS were computed for the NPF event days.

The condensable vapour source rate (Q, cm^{-3} s^{-1}) can be calculated according to Kulmala et al. (2001):

$$\mathrm{Q} = \mathrm{CS} \,.\, \mathrm{C} \qquad 10$$

where C is the condensable vapour concentration (cm^{-3}), can be calculated as follows:

$$\mathrm{C} = \mathrm{A} \,.\, \frac{\mathrm{dD_P}}{\mathrm{dt}} \qquad (11)$$

where A is a constant, (1.37×10^7 h cm^{-3} nm^{-1}).

3. Results and Discussion

3.1 Overview of the particle number concentrations

Table 4 summarizes the statistical parameters for size segregated particle number concentrations and eBC covering the entire measurement period at both sites. The particle number concentrations for the N_{nuc}, N_{Aitken}, and N_{acu} are 2002, 3528, and 1576 # cm^{-3}, at AURN site, 1455, 2407, and 874 # cm^{-3} at BF site, respectively. The particle number concentration of the Aitken mode generally dominates at both sites. This might be related to the strong impact of vehicle emissions and metrological factors on the particle number concentration of the N_{Aitken} in urban areas. Generally, the vehicles in urban area of Leicester are dominated by petrol cars and diesel buses according to the newest data of registered vehicles in Leicester City (Department of Transport of UK government, http://www.dft.gov.uk/traffic-counts, and count point 36549). Laboratory studies have demonstrated that the average diameters of particles emitted by gasoline engine vehicles range from 40 nm to 80 nm (Ristovski et al., 1998; Harris and Maricq, 2001). Those studies suggest that the particles measured within this size range are most likely associated with traffic emissions. In addition, some studies have shown that particle diameter on urban road measurements were smaller (probably smaller than 30 nm) than those observed under laboratory conditions (Wehner et al., 2002; Kittelson et al., 2004). The average size-segregated particle number concentrations in this study are compared with other European studies (see Table 5). The average concentrations of N_{nuc} and N_{Aitken} are lower than that in Leipzig, Helsinki, and London. However, they are higher than those in Copenhagen and Harwell. The average concentrations of N_{acu} are higher than those studies at AURN site, whereas they are lower than those studies except in Harwell at BF site. It should be noted that the differences might be related to the instrumentation (different size range of diameter), and also the sampling locations and weather conditions at each cities. The mean and median values of the metrological parameters are shown in Table 3. Form these values it can be suggested that the weather conditions are similar during the measurements at both sites (from March to May 2014). However, temperature is lower in March, when compared with April, and May, for instance average T are 8.84, 10.8, and 12.45 ^{o}C for March, April, and May 2014, respectively. It is clearly showed that little change in temperature (~ ±2-3 ^{o}C). It should be noted that the PNSD might also be influenced by metrological conditions during our measurements. Table 6 presents Pearson's correlation coefficients between PNSD and metrological parameters at both sites. PNSD showed no relation with all metrological parameters. The very low correlation

coefficients can be explained as a results of the local sources (such as traffic emissions) that dominate the sources of PNSD and also indicated that traffic emissions have higher impact on PNSD than metrological conditions at both sites. From these results it can be concluded that PNSD at both sites are influenced more by vehicle exhaust emissions rather than metrological conditions during our campaign.

In addition, Figure 2 shows the variability of the atmospheric particle number size distribution at two urban background sites within Leicester. The AURN site shows considerably higher particle number concentrations than the BF site. Proximity to roads is the primary driver: the distance between AURN site and the major and minor roads were 140 m and 20 m, respectively, and also to the effect of numbers of vehicles that passing by the major and busy road (see section 2.1). For particle diameters smaller than 100 nm an obvious difference in the concentrations is observed between the both sites. The small particles dominate the total particle number concentration (N_{total}) (see Table 4) at both sites. This observation is indicative of on-road traffic exhaust emissions as the main source of particles and particularly of the small particles as observed in previous studies in an urban areas (Bukowiecki et al., 2003; Wehner and Wiedensohler, 2003; Putaud et al., 2004). The number size distribution for particles greater than 200 nm is fairly similar at both sites. This size range belongs to the long-lived particles in accumulation mode. From the data in Figure 2 and Table 4 it can be suggested that sources of larger particles(> 200 nm) differ from sources of the smaller particles(<100nm); these larger particles are most likely dominated by regional background sources (Birmili et al., 2013). Moreover, the size distribution at the AURN site shows bimodal distribution at ~22 nm with a minor peak at ~70 nm(see Figure 2), which is consistent with a previous study in an urban area (Jeong et al., 2010). The size distribution at BF site, however, exhibits unimodal distribution at ~35 nm (see Figure 2), and was similar to previous studies that have observed unimodal size distribution in urban areas (Harrison et al., 1999; Krudysz et al., 2009). This difference might be indicative of the impact of vehicle exhaust particles with high instability, which might undergo rapid changes in size distribution of particles through evaporation or condensation process.

3.2 Particle number size distributions

The following sections will focus on the discussion of the measured average particle number size distribution at both sites and also its dependence on the time of the day. In addition, the impact of school holidays (Easter) on particle number at the BF site, along with weekday and weekend variations at both sites will be discussed.

3.2.1 Easter holiday

Figure 3 shows particle size distribution for three weeks (before Easter, Easter Week, and after Easter) at the BF site. To show the impact of vehicle emissions at this site three weeks data have been selected around the school holidays. Several primary, preparatory schools and day nurseries are located near the BF site. The impact of the Easter holiday period on UFP number concentration can clearly be observed, with much lower UFP concentrations during the Easter holidays. Generally, the UFP number concentrations observed during Easter holiday week were lower when compared with the week before and after the holiday. This was because of lower traffic density during Easter holiday and also because the schools are closed during Easter in Leicester. Moreover, Table 7 shows mean and median levels of the PNSD, traffic-related pollutants, and the traffic intensity to reveal the impact of traffic on PNSD in detail during Easter school holiday (14th-25th April 2014) in Leicester. It can be seen the levels of traffic-related pollutants such as NO_X, and eBC during a week (Monday-Friday) before and after are higher than the levels during the Easter holiday weeks. The average concentrations of NO_X are a 42.98, 43.91, and 31 μg m^{-3}, and eBC are 1.52, 1.45, 0.91 μg m^{-3} for week before, after, and Easter period, respectively. In addition, the traffic intensity (number of vehicles per hour) are also shown in Table 7. The lower traffic density during Easter holiday was observed when compared with the week before and after, the traffic intensity are 539, 518, and 373 vehicles h^{-1} for week before, after, and Easter period, respectively. This result showed that during Easter holiday was observed lower traffic intensity, the traffic-related pollutants, and the PNSD. This might be linked to the impact of holiday of the schools in Leicester during the Easter holiday since people have not used their cars as much as normal school days. It can be concluded that Easter holidays can impact on PNSD in Leicester.

3.2.2 Temporal Variations

Diurnal and nocturnal variations of the particle size distribution at both sites shown in Figure 4. At both sites higher concentrations were found in the nucleation mode (diameters less than 25 nm) during daytime (7:00-19:00), caused by the new particle formation events that are observed at both sites. Lower concentration of particle diameter in the size range ~30-100nm are observed during the daytime at both sites. This is probably as a result of the higher mixing layer and higher wind speed leading to better mixing of particles, which occurs mostly in spring and summer in urban background areas (Ketzel et al., 2004; Wu et al., 2008). Previous studies conducted in different areas in Sweden and Copenhagen have found similar results during daytime (Ketzel et al., 2004).

Particle number size distribution showed higher concentrations during weekdays than weekends, which is related to the influence of vehicle emissions and number of vehicles in urban areas (Morawska et al., 2002). Variations of particle size distribution between weekdays (Monday to Friday, excluding holidays) and weekends at both sites are shown in Figure 5. Generally, during weekday's higher ultrafine particle number concentrations were observed at both sites. On weekends, ultrafine particle number concentrations were lower due to lower traffic intensity. Similar results have been found in previous studies in urban areas (Morawska et al., 2002; Hussein et al., 2004). Particles greater than 100 nm in diameter did not show differences during weekdays and weekends: this suggests that these particles might be partially associated to other sources rather than vehicle exhaust emissions.

Average diurnal variations of the N_{nuc}, N_{Aitken}, N_{acu}, and N_{total} concentrations for both the sites averaged separately for weekdays and weekends are shown in Figure 6a and 6b. Statistical parameters for the four modes over the entire measurement period were calculated and tabulated in Table 4. For both sites the mean diurnal variation of N_{nuc}, N_{Aitken}, and N_{total} concentrations for workdays clearly resemble the usual activity pattern of people in cities, particularly that of traffic activity. Figure 6a and 6b show clear peaks for two modes (N_{nuc} and N_{Aitken}) in the morning between 6-8 am on weekdays, which coincide with morning traffic rush hours combined with a lower mixing layer height and lower ambient temperature. The second clear peak on working days and even on weekends, however, occurs at about 7-9pm, thus significantly later than the evening traffic rush hours, which typically occur in Leicester around 4-6pm. The late afternoon peak is more influenced by local meteorology conditions than by vehicular exhaust emissions. The influence of combustion activities and domestic heating at

evenings can also play a crucial role on increasing particle number concentration in urban area (Allan et al., 2010). The observed diurnal behaviour in the Leicester urban background is consistent with the previous studies have made in many other European cities at similarly located sites (Hussein et al., 2004; Aalto et al., 2005; Moore et al., 2007; Avino et al., 2011; Borsos et al., 2012; Dall'Osto et al., 2013). Interestingly, another clear peak was observed at midday or early afternoon and which N_{Aitken} peak which did not track as shown in Figure 6a and 6b for N_{nuc} on weekdays and even more clearly on weekends. This peak might be related to the new particle formation which typically occurs at midday when traffic intensity is quite low, and most strongly during spring or summer (Reche et al., 2011; Brines et al., 2015). The lowest concentration was observed for accumulation mode particles in the afternoon, which was mainly affected by the higher mixing layer. At the weekends, it can be seen that the morning peak occurs later compared to weekdays, associated with the tendency for people to go out later in the morning at weekends. Another high peak was also observed during evening; this is probably due to intense leisure traffic at the weekend evening.

The weekly variations of the different modes of particle number concentration at both sites are shown in Figure 7a and 7b. In general, all particle modes concentrations (except Naccu) had a weekly cycle with higher number concentrations from Monday to Saturday and lower on Sunday, because there are less traffic emissions on Sunday in Leicester. The urban traffic emissions have large impact on weekly cycle of particle number concentrations and this is one probability to separate traffic vehicle emissions from other emission sources within the city (Hussein et al., 2004; Harrison and Jones, 2005; Massling et al., 2005).

To confirm the role or otherwise of NPF in the observed afternoon peaks (see Figure 6a and 6b) diurnal variations of N_{nuc}. N_{total}, NO_X, and eBC for the NPF and non-NPF event days were averaged (see Figure 8a and 8b). Figure 8a clearly shows a peak for N_{nuc}, and N_{total}, at noon during NPF event days that confirm NPF occur at urban background sites in Leicester. It should be noted that NOx and eBC were only observed in the morning and afternoon rush hour peaks, but do no peaks at noon; confirmation that the peak at noon belongs to NPF rather than local sources (such as traffic emissions). However, during non-NPF event days the diurnal variations of N_{nuc}, N_{total}, NOx, and eBC clearly showed two peaks during morning and afternoon traffic rush hours in Leicester which belongs to the local sources and N_{nuc} follows NOx and eBC profile as presented in Figure 8b. It can be concluded that the peaks were found at noon in

Figure 6a and 6b can be related to NPF events and more clearly appeared at BF site (Figure 6b) since NPF event days at BF site happen more than AURN site in this study (Figure 6a).

3.3 Dependency on wind speed and direction

A technique that has been used with previous success for identifying emission sources is the Conditional Probability Function (CPF). The CPF is a simple, fast and effective technique for providing directional information about main pollutant sources (Uria-Tellaetxe and Carslaw, 2014; Carslaw, 2015). In addition, bivariate polar plots have been shown to be particularly valuable for recognising and understanding sources of air pollutants (Carslaw et al., 2006; Westmoreland et al., 2007). CPF plots display how a pollutant concentration varies by wind speed and direction at a receptor (Carslaw and Ropkins, 2012). Figure 9a shows a CPF plot for TNC at AURN site, representing TNC sources where the total particle number concentration (30 min averaged) is >50th percentile TNC equal to 7728 # cm^{-3}. In Figure 9a there is a clear implication that there is a higher probability of these particle concentrations originating from the north-west and south-west, corresponding to the direction of University and Welford Roads (see sampling sites in section 2.1). By comparison, Figure 9b shows a bivariate polar plot for the same TNC data period. In this plot also the most obvious feature are the higher particle concentrations of total number particles can be found at low WS (less than 2 ms^{-1}) from the same directions of the CPF plot. This behaviour would typically be expected at urban background sites where high particle number concentrations are observed in stable atmospheric environment conditions and when non-buoyant ground-level sources such as road traffic emissions and domestic heating are important sources. Figure 9c and 9d illustrate CPF and bivariate plot for eBC at the AURN site, highlighting eBC sources where the eBC concentration is >50th percentile eBC equals 1.3 µg m^{-3}. Figure 9c shows there that could be more than two major sources of eBC, when compared with the TNC plots. The maxima to the north-east indicative of residential sources (domestic heating, and wood burning sources). Moreover, Figure 9d shows a similar feature with observed high concentration of eBC at low WS. In the case of the BF site (Figure 10a and 10c), it can be seen high concentrations of TNC and eBC are dominated by north and south west wind directions, corresponding to minor and major roads (Ashfield and London Roads, for more detail see sampling sites in section 2.1) near this temporary station as well as domestic heating emissions including wood burning and cooking.

Figure 10b and 10d provides the same features as Figure 9b and 9d, showing that low concentrations are observed for 30 min averaged TNC and eBC at low WS (lower than 2 ms^{-1}). In addition, in Figure 10b and d indicate the same directions as that found in the CPF plots, showing that high concentration of TNC and eBC are originating from the major road (London Road) which lies in a north and south-west direction. Both the CPF and bivariate polar plots are useful in highlighting the dominant wind direction and source types affecting the monitoring sites.

In addition, inverse relationships between different modes of PNSD and WS are observed (Figure 11a-d and Figure 12a-d). Figure 11 shows the relationships between different modes of PNSD and WS at AURN site. It should be noted that high concentrations of PNSD were observed at low WS (< 2 m s^{-1}). This observation might be related to the dilution effect. Dilution is affected by metrological conditions such as the mixing layer height, which controls the vertical dilution, and wind direction and speed, which control horizontal dilution. The association with lower wind speeds probably relates to the balance between lower dilution at low wind speeds and the longer transport times at these lower wind speeds, which allow more time for dispersion and deposition. Similar patterns were observed at the BF site when high PNSD levels were measured during low WS as presented in Figure 12a-d. It can be concluded that the observed PNSD was dominated by local sources, rather than regional sources in Leicester urban area.

3.4 Observation of new particle formation

The general definition of a nucleation event is a period when an increase in the number concentration of nucleation mode particles occurs, and those particles begin to grow into Aitken or accumulation mode particles, typically over a few hours until they disappear into the atmosphere by condensation/coagulation sinks (Kulmala et al., 2004; Dal Maso et al., 2005). The second major source of ultrafine particles in the urban atmosphere of developed urban areas is secondary aerosol formation (Brines et al., 2015). Previous studies using measurements in Birmingham (approximately 55 km from Leicester) have shown that there are three main sources of such particles: emissions from road traffic, emissions within the plumes from stationary point sources, and secondary particle formation within urban air (Shi et al., 2001;

Alam et al., 2003). Recently, Hoffman et al (2016) simply described NPF events only at AURN site (31 days). In this study NPF events for where observed on 86 days (including AURN site data) and focused on NPF events at BF site. During the study period in Leicester a total of 14 days of NPF events (four days at the AURN site, and ten days at the BF site) were observed during the morning (after morning rush hours) and afternoon hours (before evening rush hour). This emphasises the importance of this mechanism during the spring season. This is consistent with the previous study conducted in Helsinki (Northern Europe) urban atmosphere that observed maximum photochemical particle formation during spring (Hussein et al., 2008). Figure 13a and 13b show two NPF events on different two days that were observed at BF site. In the first case (Figure 13a) three peaks were observed for TNC during the day: the first of which occurred from around 06:00 to 08:00, possibly due to traffic exhaust emissions during the morning peak hours in Leicester; the second peak was observed from around 10:30 to 15:00, probably owing to the formation of new particles; and the third one was also most likely caused by traffic exhausts emissions during the evening peak hours. The NPF event was observed clearly at around 10:30-15:00 when traffic emissions were low due to a decrease in traffic volume, but TNC was found to be high (12289 # cm^{-3}) and eBC (known as a traffic emission marker) concentrations where low (0.45 μg m^{-3}). The highest temperature was about 13.8 ºC and relative humidity was around 30-40 % at around 10:30-15:00. In the second case (Figure 13b), NPF occurred at around 12:00-13:50, in similar conditions to the previous example: TNC was found high (15516 # cm^{-3}) and eBC was low (0.33 # cm^{-3}). The temperature was similar at 14.4 ºC with a low relative humidity (40-50%). Conditions observed during these NPF events, of higher temperature and lower relative humidity, are typical as they produce the stable atmospheric condition which are the most favourable for the formation of new particles (Boy and Kulmala, 2002; Holmes, 2007; Kulmala and Kerminen, 2008). Higher mean N_{total} and N_{nuc} were found for NPF event days at 2664 # cm^{-3} and 7296 # cm^{-3}, compared to that for non-event days (1901 # cm^{-3} and 6766 # cm^{-3}) at the AURN and BF sites (see Table 8). These results suggested that the burst of nucleation mode particles encouraged by the NPF had a significant influence on the increasing particle number concentration during the campaign period at both sites.

3.5 Nucleation event characterisation

Table 9 summarises the GR, J_{10-25}, CS, Q, and relevant measurements for respective nucleation events observed in this study. The parameters (GR, J_{10-25}, CS, and Q) were calculated as described earlier. At the AURN site, the GR values varied in the range from 6.6 to 8.33 nm h^{-1} (average 7.42 nm h^{-1}), the J_{10-25} values between 0.89 and 1.82 cm^{-3} s^{-1} (average 1.3 cm^{-3} s^{-1}). At BF site, the GR values varied in the range from 1.74 to 8.77 nm h^{-1} (average 5.3 nm h^{-1}), the J_{10-25} values between 0.41 and 1.70 cm^{-3} s^{-1} (average 1.17 cm^{-3} s^{-1}). The average values of GR, and J_{10-25} at AURN site were higher than BF site, which can be explained by impact of metrological conditions From March to May at both sites. In addition, the average of GR found in this study in line with the range of typical growth rate of 1-20 nm h^{-1} (Kulmala et al., 2004).The variations in GR values were related to the metrological condition (T, and RH), and the production of condensable vapours (Yli-Juuti et al., 2011). The J_{10-25} values observed at both sites were lower than observed at other urban areas such as Helsinki (2.4 cm^{-3} s^{-1}, (Hussein et al., 2008)), Marseille (3-5.3 cm^{-3} s^{-1}, (Petäjä et al., 2007), and Budapest (4.2 cm^{-3} s^{-1}, (Salma et al., 2011)). However, the values at both sites were higher than the observations in clean environments such as Hyytiälä (0.8 cm^{-3} s^{-1}, (Dal Maso et al., 2005)), and Hohenpeissenberg (1 cm^{-3} s^{-1}, (Birmili et al., 2003)). The formation rate of nucleation mode particles is known to be influenced by the chemical and physical condition of the atmosphere. Nucleation mode particles related to traffic emissions are produced behind the exhaust tailpipe as the exhaust gases are cooled and diluted in ambient air. These particles though secondary, as they are formed close to the source, can be considered to be primary. In this study, the J_{10-25} was impacted by the primary and secondary sources in Leicester urban areas. It should be noted that the low values of J_{10-25} in this study, might be associated to the relatively high concentration of pre-existing particles in Leicester environment.

The CS average values were 5.7, and 4.53 × 10^{-3} s^{-1}, the average Q values were 5.9, and 4.23 × 10^{5} cm^{-3} s^{-1}, at AURN, and BF sites, respectively (see Table 9). The CS average values observed in this study were comparable with the other studies in European cities such as Athens (0.006 s^{-1}, (Kulmala et al., 2005)), and Helsinki (0.006 s^{-1}, (Hussein et al., 2008)). Kulmala et al. (2005) observed CS values between 1.3 × 10^{-2} and 0.6 × 10^{-4} s^{-1} in deferent locations. The CS was normally higher in more polluted areas such as New Delhi and Nanjing (2.4-7 × 10^{-2} s^{-1}, (Kulmala et al., 2005; Herrmann et al., 2014)), while the CS values in European cities (such as

Athens and Marseille) were 5-10 times lower (Kulmala et al., 2005). The CS in the rural areas is approximately two to three times lower than urban environments due to the variance in number concentrations and size distributions. The Q average values found in this study were similar with other European urban background sites ($2.6 \times 10^5 – 1.6 \times 10^6$ cm^{-3} s^{-1}, (Kulmala et al., 2005)). It can be seen that more vapours should be involved in the particle growth processes to prevent the new particle formation in a polluted urban areas as a result the high vapour source rate obtained. For example, the high source rate of condensable vapour observed in New Delhi (**(**$0.9 -1.4 \times 10^7$ cm^{-3} s^{-1}, (Kulmala et al., 2005), and North Plain China ($0.6 -2.5 \times 10^6$ cm^{-3} s^{-1}, (Wang et al., 2013). It can be seen that high hourly average O_3 levels observed during NPF events at both sites (Table 9). The mass concentrations of O_3 were higher than 60 µg m^{-3} in all days during NPF events, and reached maximum 89.98 µg m^{-3} on 3rd May 2014 (Table 9), proposing that O_3 and NPF has similar sources or formation processes and most likely the photochemical among the precursors (such as VOCs, NO_X, and SO_2) of O_3 and NPF. As such, O_3 can be a significant indicator for NPF event occurrence. In addition, O_3 can also be the precursor of NPF as it is responsible for the production of condensable compounds through direct reactions (with VOCs), and indirect formation of other oxidants (such as OH and HO_2). However, NO_X as the precursor gas in photochemistry, did not show significant correlation with NPF. The average concentrations of NO_X were found low (lower than ~22 µg m^{-3}) during NPF event days, and reached minimum (~ 9 µg m^{-3}). It might be related to the increase of solar radiation during NPF which would enhance the decline of NO_X via the complex photochemical reactions.

4. Conclusions

A SMPS was utilized for the real-time measurement of particles in the size range of 10 nm to 1093 nm, to characterize the evolution of particle number size distribution and new particle formation (NPF) events in Leicester, UK. The diurnal and weekly variations of size-segregated particle number and eBC mass concentrations were characterised. At the AURN site the N_{nuc}, N_{Aitken}, N_{accu}, N_{total}, and eBC mass concentrations were 2002, 3258, 1576, 6837 # cm^3, and 1.7 µg m^{-3}, and at the BF site 1455, 2407, 874, 4737 # cm^3, and 0.77 µg m^{-3}, respectively. N_{total} seem to be dominated mostly by the N_{nuc}, and N_{Aitken} particles at both sites, demonstrating that particles at both sites are predominantly influenced by traffic emissions. The highest N_{nuc} and N_{Aitken} were observed during workdays, and the lowest concentrations observed during weekends, especially Sundays. The temporal variation of N_{accu} was not significant. The diurnal variation of the N_{total}, eBC, and NO_X concentrations demonstrated very similar behaviour at both sites, with the maximum concentrations occurring during morning and late evening hours and the lowest variation during the afternoon hours. This behaviour could be attributed to primary emissions of ultrafine particles (e.g. traffic) and the temporal evolution of mixing layer. According to wind polar plots it can be observed that more particles come from the directions that the busy roads and residential areas in the vicinity, suggesting that aerosol particles originate mainly from traffic and domestic heating emissions. Finally, this short-term study has shown that ultrafine particles are increased by NPF events at both sites; however, not enough to conclude that new particle formation is a major source of atmospheric particles in Leicester. In order to be able to reveal the impact of NPF on ultrafine particles longer term measurements of PNSD in Leicester would be necessary.

Acknowledgements

The authors would like to thank the Human Capacity Development Program from the Kurdistan Government for a scholarship (S. M. L. HAMA). We would like also to thank Dr Jolanta Obszynska (Leicester City Council) for providing meteorological data. This research was funded by the Joint Air Quality Initiative (JOAQUIN) project, part of the EU Interreg IV-B NWE Program.

References

Aalto, P.P., Hämeri, K., Paatero, P., Kulmala, M., Bellander, T., Berglind, N., Bouso, L., Castaño-Vinyals, G., Sunyer, J., Cattani, G., Marconi, A., Cyrys, J., Klot, S., Peters, A., Zetzsche, K., Lanki, T., Pekkanen, J., Nyberg, F., Sjövall, B. and Forastiere, F. (2005). Aerosol Particle Number Concentration Measurements in Five European Cities Using Tsi-3022 Condensation Particle Counter over a Three-Year Period During Health Effects of Air Pollution on Susceptible Subpopulations. *Journal of the Air & Waste Management Association* 55: 1064-1076.

Agus, E.L., Young, D.T., Lingard, J.J., Smalley, R.J., Tate, J.E., Goodman, P.S. and Tomlin, A.S. (2007). Factors Influencing Particle Number Concentrations, Size Distributions and Modal Parameters at a Roof-Level and Roadside Site in Leicester, Uk. *The Science of the total environment* 386: 65-82.

Alam, A., Shi, J.P. and Harrison, R.M. (2003). Observations of New Particle Formation in Urban Air. *Journal of Geophysical Research: Atmospheres* 108: n/a-n/a.

Allan, J.D., Alfarra, M.R., Bower, K.N., Coe, H., Jayne, J.T., Worsnop, D.R., Aalto, P.P., Kulmala, M., Hyotylainen, T., Cavalli, F., and and Laaksonen, A. (2010). Size and Composition Measurements of Background Aerosol and New Particle Growth in a Finnish Forest During Quest 2 Using an Aerodyne Aerosol Mass Spectrometer. *Atmos. Chem. Phys.* 6: 315-327.

Avino, P., Casciardi, S., Fanizza, C. and Manigrasso, M. (2011). Deep Investigation of Ultrafine Particles in Urban Air. *Aerosol and Air Quality Research* 11: 654-663.

Birmili, W., Beeresheim, H., Plass-Dulmer, C., Elste, T., Gigle, S., Wiedensohler, A. and Uhrner, U. (2003). The Hohenpeissenberg Aerosol Formation Experiment (Hafex): A Long-Term Study Including Size-Resolved Aerosol, H2so4, Oh, and Monoterpenes Measurements. *Atmos. Chem. Phys.* 3: 361-376.

Birmili, W., Tomsche, L., Sonntag, A., Opelt, C., Weinhold, K., Nordmann, S. and Schmidt, W. (2013). Variability of Aerosol Particles in the Urban Atmosphere of Dresden (Germany): Effects of Spatial Scale and Particle Size. *Meteorologische Zeitschrift* 22: 195-211.

Boogaard, H., Kos, G.P.A., Weijers, E.P., Janssen, N.A.H., Fischer, P.H., van der Zee, S.C., de Hartog, J.J. and Hoek, G. (2011). Contrast in Air Pollution Components between Major Streets and Background Locations: Particulate Matter Mass, Black Carbon, Elemental Composition, Nitrogen Oxide and Ultrafine Particle Number. *Atmospheric Environment* 45: 650-658.

Borsos, T., Rimnacova, D., Zdimal, V., Smolik, J., Wagner, Z., Weidinger, T., Burkart, J., Steiner, G., Reischl, G., Hitzenberger, R., Schwarz, J. and Salma, I. (2012). Comparison of Particulate Number Concentrations in Three Central European Capital Cities. *The Science of the total environment* 433: 418-426.

Boy, M.a. and Kulmala, M. (2002). Nucleation Events in the Continental Boundary Layer: Influence of Physical and Meteorological Parameters. *Atmos. Chem. Phys.* 2: 1-16.

Brines, M., Dall'Osto, M., Beddows, D.C.S., Harrison, R.M., Gómez-Moreno, F., Núñez, L., Artíñano, B., Costabile, F., Gobbi, G.P., Salimi, F., Morawska, L., Sioutas, C. and Querol, X. (2015). Traffic and Nucleation Events as Main Sources of Ultrafine Particles in High-Insolation Developed World Cities. *Atmospheric Chemistry and Physics* 15: 5929-5945.

Bukowiecki, N., Dommen, J., Prevot, A.S.H., Weingartner, E.a. and Baltensperger, U. (2003). Fine and Ultrafine Particles in the Z¨ Urich (Switzerland) Area Measured with a Mobile Laboratory. An Assessment of the Seasonal and Regional Variation Throughout a Year. *Atmos. Chem. Phys. Discuss* 3: 2739-2782.

Butterfield, D., Beccaceci, S., Quincey, P., Sweeney, B., Lilley, A., Bradshaw, C., Fuller, G., Green, D. and Font Font, A. (2015). 2014 Annual Report for the Uk Black Carbon Network, National Physical Laboratory. Hampton Road, Teddington, Middlesex, TW11 0LW, Queen's Printer and Controller of HMSO,.

Carslaw, D.C. (2015). The Openair Manual — Open-Source Tools for Analysing Air Pollution Data., In *Manual for version 1.5-9*, King's College London.

Carslaw, D.C., Beevers, S., Ropkins, K. and Bell, M. (2006). Detecting and Quantifying Aircraft and Other on-Airport Contributions to Ambient Nitrogen Oxides in the Vicinity of a Large International Airport. *Atmospheric Environment* 40: 5424-5434.

Carslaw, D.C. and Ropkins, K. (2012). Openair — an R Package for Air Quality Data Analysis. *Environmental Modelling & Software.* 27-28: 52-61.

Charron, A., Birmili, W. and Harrison, R.M. (2007). Factors Influencing New Particle Formation at the Rural Site, Harwell, United Kingdom. *Journal of Geophysical Research* 112.

Cordell, R.L., Mazet, M., Dechoux, C., Hama, S.M.L., Staelens, J., Hofman, J., Stroobants, C., Roekens, E., Kos, G.P.A., Weijers, E.P., Frumau, K.F.A., Panteliadis, P., Delaunay, T., Wyche, K.P. and Monks, P.S. (2016). Evaluation of Biomass Burning across North West Europe and Its Impact on Air Quality. *Atmospheric Environment* 141: 276-286.

Dal Maso, M., Kulmala, M., Lehtinen, K.E., Makela¨ , J.M., Aalto, P.P. and O'Dowd, C. (2002). Condensation and Coagulation Sinks and Formation of Nucleation Mode Particles in Coastal and Boreal Forest Boundary Layers. *GEOPHYSICAL RESEARCH* 107: 1-10.

Dal Maso, M., Kulmala, M., Riipinen, I., Wagner, R., Hussein, T., Aalto, P.P. and Lehtinen, K.E.J. (2005). Formation and Growth of Fresh Atmospheric Aerosols: Eight Years of Aerosol Size Distribution Data from Smear Ii, Hyytiälä, Finland. *Boreal Env. Res.* 10: 323-336.

Dall'Osto, M., Querol, X., Alastuey, A., O'Dowd, C., Harrison, R.M., Wenger, J. and Gómez-Moreno, F.J. (2013). On the Spatial Distribution and Evolution of Ultrafine Particles in Barcelona. *Atmospheric Chemistry and Physics* 13: 741-759.

Dall'Osto, M., Thorpe, A., Beddows, D.C.S., Harrison, R.M., Barlow, J.F., Dunbar, T., Williams, P.I. and Coe, H. (2011). Remarkable Dynamics of Nanoparticles in the Urban Atmosphere. *Atmospheric Chemistry and Physics* 11: 6623-6637.

Fruin, S., Westerdahl, D., Sax, T., Sioutas, C. and Fine, P.M. (2008). Measurements and Predictors of on-Road Ultrafine Particle Concentrations and Associated Pollutants in Los Angeles. *Atmospheric Environment* 42: 207-219.

Hama, S.M.L., Ma, N., Cordell, R.L., Kos, G.P.A., Wiedensohler, A. and Monks, P.S. (2017). Lung Deposited Surface Area in Leicester Urban Background Site/Uk: Sources and Contribution of New Particle Formation. *Atmospheric Environment* 151: 94-107.

Harris, S.J. and Maricq, M.M. (2001). Signature Size Distributions for Diesel and Gasoline Engine Exhaust Particulate Matter. *Aerosol Science* 32: 749-764.

Harrison, R.M. and Jones, A.M. (2005). Multisite Study of Particle Number Concentrations in Urban Air. *Environ. Sci. Technol.* 39: 6063-6070.

Harrison, R.M., Jones, A.M. and Lawrence, R.G. (2004). Major Component Composition of Pm10 and Pm2.5 from Roadside and Urban Background Sites. *Atmospheric Environment* 38: 4531-4538.

Harrison, R.M., Jones, M. and Collins, G. (1999). Measurements of the Physical Properties of Particles in the Urban Atmosphere. *Atmospheric Environment* 33: 309-321.

Herrmann, E., Ding, A.J., Kerminen, V.M., Petäjä, T., Yang, X.Q., Sun, J.N., Qi, X.M., Manninen, H., Hakala, J., Nieminen, T., Aalto, P.P., Kulmala, M. and Fu, C.B. (2014). Aerosols and Nucleation in Eastern China: First Insights from the New Sorpes-Nju Station. *Atmospheric Chemistry and Physics* 14: 2169-2183.

Hinds, W.C. (1999). *Aerosol Technology: Properties, Behavior, and Measurement of Airborne Particles* 2nd ed, JOHN WILEY & SONS, INC., Canada.

Hofman, J., Staelens, J., Cordell, R., Stroobants, C., Zikova, N., Hama, S.M.L., Wyche, K.P., Kos, G.P.A., Van Der Zee, S., Smallbone, K.L., Weijers, E.P., Monks, P.S. and Roekens, E. (2016). Ultrafine Particles in Four European Urban Environments: Results from a New Continuous Long-Term Monitoring Network. *Atmospheric Environment* 136: 68-81.

Holmes, N.S. (2007). A Review of Particle Formation Events and Growth in the Atmosphere in the Various Environments and Discussion of Mechanistic Implications. *Atmospheric Environment* 41: 2183-2201.

Hussein, T., Martikainen, J., Junninen, H., Sogacheva, L., Wagner, R., Dal Maso, M., Riipinen, I., Aalto, P.P., and and Kulmala, M. (2008). Observation of Regional New Particle Formation in the Urban Atmosphere. *Tellus B* 60: 509-521.

Hussein, T., Puustinen, A., Aalto, P.P., Ma¨kela¨ , J.M., Ha¨meri, K. and Kulmala, M. (2004). Urban Aerosol Number Size Distributions. *Atmos. Chem. Phys.* 4: 391-411.

Ingrid Sundvor, N.C.B., Mar Viana, Xavier Querol, Cristina Reche, Fulvio Amato, Giorgos Mellios, Cristina Guerreiro (2012). Road Traffic's Contribution to Air Quality in European Cities. *The European Topic Centre on Air Pollution and Climate Change Mitigation*

Invernizzi, G., Ruprecht, A., Mazza, R., De Marco, C., Močnik, G., Sioutas, C. and Westerdahl, D. (2011). Measurement of Black Carbon Concentration as an Indicator of Air Quality Benefits of Traffic Restriction Policies within the Ecopass Zone in Milan, Italy. *Atmospheric Environment* 45: 3522-3527.

Jeong, C.-H., Hopke, P.K., Chalupa, D. and Utell, M. (2004). Characteristics of Nucleation and Growth Events of Ultrafine Particles Measured in Rochester, Ny. *Environmental science & technology* 38: 1933-1940.

Jeong, C.H., Evans, G.J., McGuire, M.L., Chang, R.Y.W., Abbatt, J.P.D., Zeromskiene, K., Mozurkewich, M., Li, S.M. and Leaitch, W.R. (2010). Particle Formation and Growth at Five Rural and Urban Sites. *Atmospheric Chemistry and Physics* 10: 7979-7995.

Joaquin (2015). Monitoring of Ultrafine Particles and Black Carbon. Joint Air Quality Initiative, Work Package 1 Action 1 and 3., Flanders Environment Agency, Aalst.

Ketzel, M., Wahlin, P., Kristensson, A., Swietlicki, E., Berkowicz, R., Nielsen, O.J. and Palmgren, F. (2004). Particle Size Distribution and Particle Mass Measurements at Urban, near-City and Rural Level in the Copenhagen Area and Southern Sweden. *Atmos. Chem. Phys.* 4: 281-292.

Kittelson, D.B., Watts, W.F. and Johnson, J.P. (2004). Nanoparticle Emissions on Minnesota Highways. *Atmospheric Environment* 38: 9-19.

Krudysz, M., Moore, K., Geller, M., Sioutas, C.a. and Froines, J. (2009). Intra-Community Spatial Variability of Particulate Matter Size Distributions in Southern California/Los Angeles. *Atmos. Chem. Phys.* 9: 1061-1075.

Kulmala, M., Dal Maso, M., Mekela, J., M., Pirjola, L., Vekeva, M., Aalto, P.P., Miikkulainen, P., Hamer, K. and O'Dowd, C. (2001). On the Formation, Growth and Composition of Nucleation Mode Particles. *Tellus B* 53: 479-490.

Kulmala, M. and Kerminen, V.M. (2008). On the Formation and Growth of Atmospheric Nanoparticles. *Atmospheric Research* 90: 132-150.

Kulmala, M., Petäjä, T., Monkkonen, P., Koponen, K., I., Dal Maso, M., Aalto, P., Lehtinen, K.E. and Kerminen, V.M. (2005). On the Growth of Nucleation Mode Particles: Source Rates of Condensable Vapor in Polluted and Clean Environments. *Atmos. Chem. Phys.* 5: 409-416.

Kulmala, M., Petaja, T., Nieminen, T., Sipila, M., Manninen, H.E., Lehtipalo, K., Dal Maso, M., Aalto, P.P., Junninen, H., Paasonen, P., Riipinen, I., Lehtinen, K.E., Laaksonen, A. and Kerminen, V.M. (2012). Measurement of the Nucleation of Atmospheric Aerosol Particles. *Nat Protoc* 7: 1651-1667.

Kulmala, M., Vehkamäki, H., Petäjä, T., Dal Maso, M., Lauri, A., Kerminen, V.M., Birmili, W. and McMurry, P.H. (2004). Formation and Growth Rates of Ultrafine Atmospheric Particles: A Review of Observations. *Journal of Aerosol Science* 35: 143-176.

Kumar, P., Fennell, P. and Britter, R. (2008). Measurements of Particles in the 5-1000 Nm Range Close to Road Level in an Urban Street Canyon. *The Science of the total environment* 390: 437-447.

Lehtinen, K.E., Korhonen, H., Dal Maso, M. and Kulmala, M. (2003). On the Concept of Condensation Sink Diameter. *Boreal Environment Research* 8: 405-411.

Li, N., Sioutas, C., Cho, A., Schmitz, D., Misra, C., Sempf, J., Wang, M., Oberley, T., Froines, J. and Nel, A. (2002). Ultrafine Particulate Pollutants Induce Oxidative Stress and Mitochondrial Damage. *Environmental Health Perspectives* 111: 455-460.

Lohmann , U. and Feichter, J. (2005). Global Indirect Aerosol Effects: A Review. *Atmos. Chem. Phys.* 5: 715-737.

Longley, I.D., Gallagher, M.W., Dorsey, J.R., Flynn, M., Allan, J.D., Alfarra, M.R. and Inglis, D. (2003). A Case Study of Aerosol (4.6nm<Dp<10μm) Number and Mass Size Distribution Measurements in a Busy Street Canyon in Manchester, Uk. *Atmospheric Environment* 37: 1563-1571.

Massling, A., Stock, M. and Wiedensohler, A. (2005). Diurnal, Weekly, and Seasonal Variation of Hygroscopic Properties of Submicrometer Urban Aerosol Particles. *Atmospheric Environment* 39: 3911-3922.

Moore, K.F., Ning, Z., Ntziachristos, L., Schauer, J.J. and Sioutas, C. (2007). Daily Variation in the Properties of Urban Ultrafine Aerosol—Part I: Physical Characterization and Volatility. *Atmospheric Environment* 41: 8633-8646.

Morawska, L., Jayaratnea, E.R., Mengersenb, K., Jamriskaa, M. and Thomas, S. (2002). Differences in Airborne Particle and Gaseous Concentrations in Urban Air between Weekdays and Weekends. *Atmospheric Environment* 36: 4375-4383.

Nel, A. (2005). Air Pollution-Related Illness: Effects of Particles. 308: 804–806.

Penttinen, P., Timonen, K.L., Tiittanen, P., Mirme, A., Ruuskanen, J. and Pekkanen, J. (2001). Number Concentration and Size of Particles in Urban Air: Effects on Spirometric Lung Function in Adult Asthmatic Subjects. *Environ. Health Perspect* 109: 319-323.

Pérez, N., Pey, J., Cusack, M., Reche, C., Querol, X., Alastuey, A. and Viana, M. (2010). Variability of Particle Number, Black Carbon, and Pm10, Pm2.5, and Pm1levels and Speciation: Influence of Road Traffic Emissions on Urban Air Quality. *Aerosol Science and Technology* 44: 487-499.

Petäjä, T., Kerminen, V.M., Dal Maso, M., Junninen, H., Koponen, K., I., Hussein, T., Aalto, P.P., Andronopoulos, S., Robin, D., Hameri, K., Bartzis, J., G. and Kulmala, M. (2007). Sub-Micron Atmospheric Aerosols in the Surroundings of Marseille and Athens: Physical Characterization and New Particle Formation. *Atmos. Chem. Phys.* 7: 2705-2720.

Peters, A., Wichmann, H.E., Tuch, T., Heinrich, J. and Heyder, J. (1997). Respiratory Effects Are Associated with the Number of Ultrafine Particles. *Am. J. Respir. Crit. Care Med* 155: 1376-1383.

Petzold, A., Ogren, J.A., Fiebig, M., Laj, P., Li, S.M., Baltensperger, U., Holzer-Popp, T., Kinne, S., Pappalardo, G., Sugimoto, N., Wehrli, C., Wiedensohler, A. and Zhang, X.Y. (2013). Recommendations for Reporting "Black Carbon" Measurements. *Atmospheric Chemistry and Physics* 13: 8365-8379.

Pirjola, L., Kulmala, M., Wilck, M., Bischoff, A., Stratmann, F. and Otto, E. (1999). Formation of Sulphuric Acid Aerosols and Cloud Condensation Nuclei: An Expression for Significant Nucleation and Model Comparison. *J. Aerosol Sci.* 30: 1079-1094.

Pope, C.A. (2000). Review: Epidemiological Basis for Particulate Air Pollution Health Standards. *Aerosol Science and Technology* 32: 4-14.

Pope, C.A.I. and Dockery, D.W. (2006). Health Effects of Fine Particulate Air Pollution: Lines That Connect. *J. Air Waste Ma.* 56: 709-742.

Putaud, J.P., Raes, F., Van Dingenen, R., Brüggemann, E., Facchini, M.C., Decesari, S., Fuzzi, S., Gehrig, R., Hüglin, C., Laj, P., Lorbeer, G., Maenhaut, W., Mihalopoulos, N., Müller, K., Querol, X., Rodriguez, S., Schneider, J., Spindler, G., Brink, H., Tørseth, K. and Wiedensohler, A. (2004). A European Aerosol Phenomenology—2: Chemical Characteristics of Particulate Matter at Kerbside, Urban, Rural and Background Sites in Europe. *Atmospheric Environment* 38: 2579-2595.

R Core Team, D. R: A Language and Environment for Statistical Computing., Available at: www.R-project.org, Last Access:

Reche, C., Querol, X., Alastuey, A., Viana, M., Pey, J., Moreno, T., Rodríguez, S., González, Y., Fernández-Camacho, R., de la Rosa, J., Dall'Osto, M., Prévôt, A.S.H., Hueglin, C., Harrison, R.M. and Quincey, P. (2011). New Considerations for Pm, Black Carbon and Particle Number Concentration for Air Quality Monitoring across Different European Cities. *Atmospheric Chemistry and Physics* 11: 6207-6227.

Ristovski, Z.D., Morawska, L., Bofinger, N.D. and Hitchins, J. (1998). Submicrometer and Supermicrometer Particulate Emission from Spark Ignition Vehicles. *Environmental science & technology* 32: 3845-3852.

Rodríguez, S. and Cuevas, E. (2007). The Contributions of "Minimum Primary Emissions" and "New Particle Formation Enhancements" to the Particle Number Concentration in Urban Air. *Journal of Aerosol Science* 38: 1207-1219.

Salma, I., Borsós, T., Weidinger, T., Aalto, P., Hussein, T., Dal Maso, M. and Kulmala, M. (2011). Production, Growth and Properties of Ultrafine Atmospheric Aerosol Particles in an Urban Environment. *Atmospheric Chemistry and Physics* 11: 1339-1353.

Seinfeld, J.H. and Pandis, S.N. (1998). *Atmospheric Chemistry and Physics*, John Wiley & Sons, Inc, New York.

Seinfeld, J.H. and Pandis, S.N., , (2006). *Atmospheric Chemistry and Physics: From Air Pollution to Climate Change*, second ed. ed, John Wiley and Sons. Inc, New York.

.

Shi, J.P., Evans, D.E., Khan, A.A. and Harrison, R.M. (2001). Sources and Concentration of Nanoparticles ((10nm Diameter) in the Urban Atmosphere. *Atmospheric Environment* 35: 1193-1202.

Smargiassi, A., Baldwin, M., Pilger, C., Dugandzic, R. and Brauer, M. (2005). Small-Scale Spatial Variability of Particle Concentrations and Traffic Levels in Montreal: A Pilot Study. *The Science of the total environment* 338: 243-251.

Stanier, C.O., Khlystov, A.Y. and Pandis, S.N. (2004). Ambient Aerosol Size Distributions and Number Concentrations Measured During the Pittsburgh Air Quality Study (Paqs). *Atmospheric Environment* 38: 3275-3284.

Stevens, B. and Feingold, G. (2009). Untangling Aerosol Effects on Clouds and Precipitation in a Buffered System. *Nature* 461: 607-613.

Tuch, T.M., Wehner, B., Pitz, M., Cyrys, J., Heinrich, J., Kreyling, W.G., Wichmann, H.E. and Wiedensohler, A. (2003). Long-Term Measurements of Size-Segregated Ambient Aerosol in Two German Cities Located 100km Apart. *Atmospheric Environment* 37: 4687-4700.

Uria-Tellaetxe, I. and Carslaw, D.C. (2014). Conditional Bivariate Probability Function for Source Identification. *Environmental Modelling & Software* 59: 1-9.

von Bismarck-Osten, C., Birmili, W., Ketzel, M., Massling, A., Petäjä, T. and Weber, S. (2013). Characterization of Parameters Influencing the Spatio-Temporal Variability of Urban Particle Number Size Distributions in Four European Cities. *Atmospheric Environment* 77: 415-429.

Wang, H., Zhu, B., Shen, L., An, J., Yin, Y. and Kang, H. (2014). Number Size Distribution of Aerosols at Mt. Huang and Nanjing in the Yangtze River Delta, China: Effects of Air Masses and Characteristics of New Particle Formation. *Atmospheric Research* 150: 42-56.

Wang, Z.B., Hu, M., Sun, J.Y., Wu, Z.J., Yue, D.L., Shen, X.J., Zhang, Y.M., Pei, X.Y., Cheng, Y.F. and Wiedensohler, A. (2013). Characteristics of Regional New Particle Formation in Urban and Regional Background Environments in the North China Plain. *Atmospheric Chemistry and Physics* 13: 12495-12506.

Wehner, B., Birmili, W., Gnauk, T. and Wiedensohler, A. (2002). Particle Number Size Distributions in a Street Canyon and Their Transformation into the Urban-Air Background: Measurements and a Simple Model Study. *Atmospheric Environment* 36: 2215-2223.

Wehner, B. and Wiedensohler, A. (2003). Long Term Measurements of Submicrometer Urban Aerosols: Statistical Analysis for Correlations with Meteorological Conditions and Trace Gases. *Atmos. Chem. Phys.* 3: 867-879.

Westmoreland, E.J., Carslaw, N., Carslaw, D.C., Gillah, A. and Bates, E. (2007). Analysis of Air Quality within a Street Canyon Using Statistical and Dispersion Modelling Techniques. *Atmospheric Environment* 41: 9195-9205.

Willeke, K. (1976). Temperature Dependence of Particle Slip in a Gaseous Medium. *Journal of Aerosol Science* 7: 381-387.

Wu, Z., Hu, M., Lin, P., Liu, S., Wehner, B. and Wiedensohler, A. (2008). Particle Number Size Distribution in the Urban Atmosphere of Beijing, China. *Atmospheric Environment* 42: 7967-7980.

Yli-Juuti, T., Nieminen, T., Hirsikko, A., Aalto, P.P., Asmi, E., Hõrrak, U., Manninen, H.E., Patokoski, J., Dal Maso, M., Petäjä, T., Rinne, J., Kulmala, M. and Riipinen, I. (2011). Growth Rates of Nucleation Mode Particles in Hyytiälä During 2003&Minus;2009: Variation with Particle Size, Season, Data Analysis Method and Ambient Conditions. *Atmospheric Chemistry and Physics* 11: 12865-12886.

Zhu, B., Wang, H., Shen, L., Kang, H. and Yu, X. (2013). Aerosol Spectra and New Particle Formation Observed in Various Seasons in Nanjing. *Advances in Atmospheric Sciences* 30: 1632-1644.

Table 1: Summary of previous PNSD studies at various UK sites.

Site	Size range (nm)	Study
Urban background site (London)	10-415	Rodríguez and Cuevas (2007)
Road site (London)	14.6-661.2	Dall'Osto et al. (2011)
Urban background site (London)	8-700	von Bismarck-Osten et al. (2013)
Road site (London)	19.2-600	von Bismarck-Osten et al. (2013)
Urban background site (Birmingham)	10-1000	Harrison et al. (1999)
Road site (Birmingham)	9.47-359	Shi et al. (2001)
Road site (Manchester)	4-160	Longley et al. (2003)
Rural site (Harwell)	11-450	Charron et al. (2007)
Urban background site (Cambridge)	10-2500	Kumar et al. (2008)
Road site (Leicester)	5-1000	(Agus et al., 2007)
AURN urban background (Leicester)	10-1093	This study
BF urban background (Leicester)	10-1093	This study

Table 2: Overview of instrument types per sampling site (March-June 2014)

Station	Location	Meteorological Parameters	W-CPC	SMPS	NOx	O_3	MAAP
AURN	UoL	-	x	-	x	x	x
Trailer (Mobile Campaign)	UoL and BF	x	x	x	-	-	x

1

2 Table 3: Mean, Median, and Max of the Metrological parameters at AURN and BF sites.

site	WS (m s^{-1})			WD (º)			T(ºC)			RH (%)		
AURN	Mean	Median	Max	Mean	Median	Max	Mean	Median	Max	Mean	Median	Max
March	1.44	1.21	9.44	176	186	329	8.8	8.84	18.5	73.9	76.6	93.95
BF												
April	1.3	1.24	4.85	175	189	313	10.76	10.8	19.1	71.4	74.41	92.44
May	0.99	1.15	3.91	192	205	305	11.7	12.45	23.75	71.55	70	92.11

3

4

5 Table 4: Summary statistics of size-segregated particle number concentrations (# cm^{-3}), and
6 eBC (µgm^{-3}).

Site	Mode	Mean	50th percentile	75th percentile	Standard deviation	Validated data
AURN	N_{nuc}	2002	1522	2612	1828	4345
	N_{Aitken}	3258	2553	3897	2646	4345
	N_{acu}	1576	1174	2073	1403	4345
	N_{total}	6837	5680	8446	4549	4345
	eBC	1.7	1.27	1.97	1.67	4308
BF	N_{nuc}	1455	1131	1878	1313	6714
	N_{Aitken}	2407	2021	3124	1513	6714
	N_{acu}	874	742	1178	548	6714
	N_{total}	4737	4250	5899	2514	6714
	eBC	0.77	0.67	0.96	0.51	7344

7

Table 5: Comparisons of size-resolved particle number concentrations (cm^{-3}) between this study and a range of other European studies. (Size range in the units of nm)

Location	N_{nuc}	N_{Aitken}	N_{acu}	Ntotal	Study
Leipzig	9850 (3-20)	9413 (20-100)	2107 (100-1000)	21377 (3-2500)	Wehner and Wiedensohler (2003)
Leipzig	4495 (8-30)	3287 (30-100)	1632 (100-700)	9398 (8-700)	von Bismarck-Osten et al. (2013)
Helsinki	7100 (8-30)	6320 (20-100)	960 (90-400)	14500 (8-400)	Hussein et al. (2004)
Helsinki	3080 (8-30)	3099 (30-100)	1053 (100-700)	7231 (8-700)	von Bismarck-Osten et al. (2013)
London	1632 (19-30)	3825 (30-100)	1437 (100-600)	6680 (19-600)	von Bismarck-Osten et al. (2013)
Copenhagen	1294 (8-30)	2994 (30-100)	984 (100-700)	5287 (8-700)	(von Bismarck-Osten et al., 2013)
Harwell	944 (11-30)	1770 (30-100)	628 (100-450)	3342 (11-450)	Charron et al. (2007)
Leicester (AURN site)	2002 (10-25)	3258 (25-100)	1756 (100-1093)	6837 (10-1093)	This study
Leicester (BF site)	1455 (10-25)	2407 (25-100)	874 (100-1093)	4737 (10-1093)	This study

Table 6: Pearson correlation coefficients between PNSD (# cm^{-3}), and the metrological parameters (WS ($m\ s^{-1}$), WD (knot), T (^{O}C), RH (%)) at AURN and BF sites.

site	Parameters	N_{nuc}	N_{Aitken}	N_{accu}	N_{total}
AURN	WS	-0.13	-0.182	-0.187	-0.216
	T	-0.055	-0.182	-0.0423	-0.141
	RH	-0.0786	0.179	0.183	0.129
BF	WS	-0.0685	-0.458	-0.340	-0.392
	T	-0.0311	-0.201	0.152	-0.105
	RH	-0.249	-0.029	-0.055	-0.015

Table 7: Mean, and Median, of the NO_X ($\mu g\ m^{-3}$), eBC ($\mu g\ m^{-3}$), PNSD (# cm^{-3}), and Traffic (vehicles h^{-1}) at BF site Week before, Easter and Week after Easter holiday 2014.

	Mean						Median					
Parameters	NOx	eBC	N_{nuc}	N_{Aitken}	N_{acu}	Traffic	NOx	eBC	N_{nuc}	N_{Aitken}	N_{acu}	Traffic
Week Before	42.98	1.52	2376	2796	592	539	39.7	1.3	2269	2386	502	651
Easter	31	0.91	821	1856	805	373	27.7	0.86	696	1605	752	460
Week After	43.91	1.45	2147	2339	668	518	38.6	1.25	1956	2182	627	669

Table 8: Statistics of particle number concentrations measured during NPF and non-NPF event days.

	Particle Modes(# cm^{-3})	Average	Median	95th percentile	S.D	No. of data
AURN Site						
NPF event days	N_{total}	2664.46	2015.81	6854.40	2049.34	576
	N_{acu}	3475.54	2941.80	8062.99	2378.40	576
	N_{Aitken}	1156.97	855.26	3078.42	932.75	576
	N_{nuc}	7296.97	6422.40	14884.28	3956.60	576
Non-event days	N_{total}	1901.35	1450.25	4638.22	1770.93	3769
	N_{acu}	3225.20	2499.52	7763.36	2683.30	3769
	N_{Aitken}	1640.14	1279.21	3885.43	1451.48	3769
	N_{nuc}	6766.69	5554.72	14856.55	4629.36	3769
BF Site						
NPF event days	N_{total}	1994.73	1593.26	4923.37	1550.02	1565
	N_{acu}	2630.39	2094.65	6363.31	1841.13	1565
	N_{Aitken}	727.84	567.77	1782.82	542.16	1565
	N_{nuc}	5352.96	4808.56	10831.69	2855.65	1565
Non-event days	N_{total}	1259.41	993.71	3128.39	1185.40	4862
	N_{acu}	2382.56	2046.61	4670.57	1396.45	4862
	N_{Aitken}	948.67	824.24	1919.25	537.58	4862
	N_{nuc}	4590.63	4169.04	8766.80	2385.92	4862

Table 9: Summary of N_{total} (# cm^{-3}), and N_{nuc} (# cm^{-3}), O_3 (µg m^{-3}), NO_X (µg m^{-3}), and NPF event characteristics (GR (nm h^{-1}), J_{10-25} (cm^{-3} s^{-1}), CS (10^{-3} s^{-1}), Q (10^{5} cm^{-3} s^{-1})) during the NPF event days.

Site	Event date	Start	End	GR	J_{10-25}	CS	Q	N_{total}	N_{nuc}	O_3	NO_X
AURN	07/03/2014	11:20	14:00	8.33	1.10	5	5.8	8582	5922	68.7	22.2
	15/03/2014	11:40	13:00	8.1	1.40	5.4	6.1	5246	3567	67.05	18.64
	16/03/2014	12:30	14:20	6.6	1.82	5.7	5.2	8264	6147	68.69	17.67
	24/03/2014	09:50	11:20	6.66	0.89	7	6.5	8720	6193	61.64	18.95
BF	08/04/2014	12:20	13:40	5.4	1.27	1.8	1.35	5418	4108	69.5	22.36
	11/04/2014	10:00	12:30	4.9	1.46	3.1	2.8	6525	4934	70.89	21.29
	27/04/2014	12:00	13:50	4.7	1.40	3.4	3	5456	4322	73.59	9.24
	02/05/2014	10:00	12:30	1.74	0.70	7.8	6.5	5742	9303	74.8	18.4
	03/05/2014	10:30	15:00	5.6	0.41	6.3	7.29	6685	4468	89.98	9.33
	07/05/2014	11:30	13:50	4.27	0.83	4.53	3.7	8222	6008	64.24	21.73
	09/05/2014	12:00	13:10	5.8	0.89	2.56	2.1	5155	3898	62.65	20.84
	10/05/2014	12:20	13:50	7.23	1.70	2.72	2.73	10927	9783	65.38	21.33
	14/05/2014	10:40	12:10	8.77	1.45	5.4	6.6	6802	4060	69.69	22.68
	17/05/2014	10:10	12:20	4.1	1.62	7.7	6.3	6037	4816	79.77	22.78

Figure 1: Map of Leicester and locations of the sampling sites

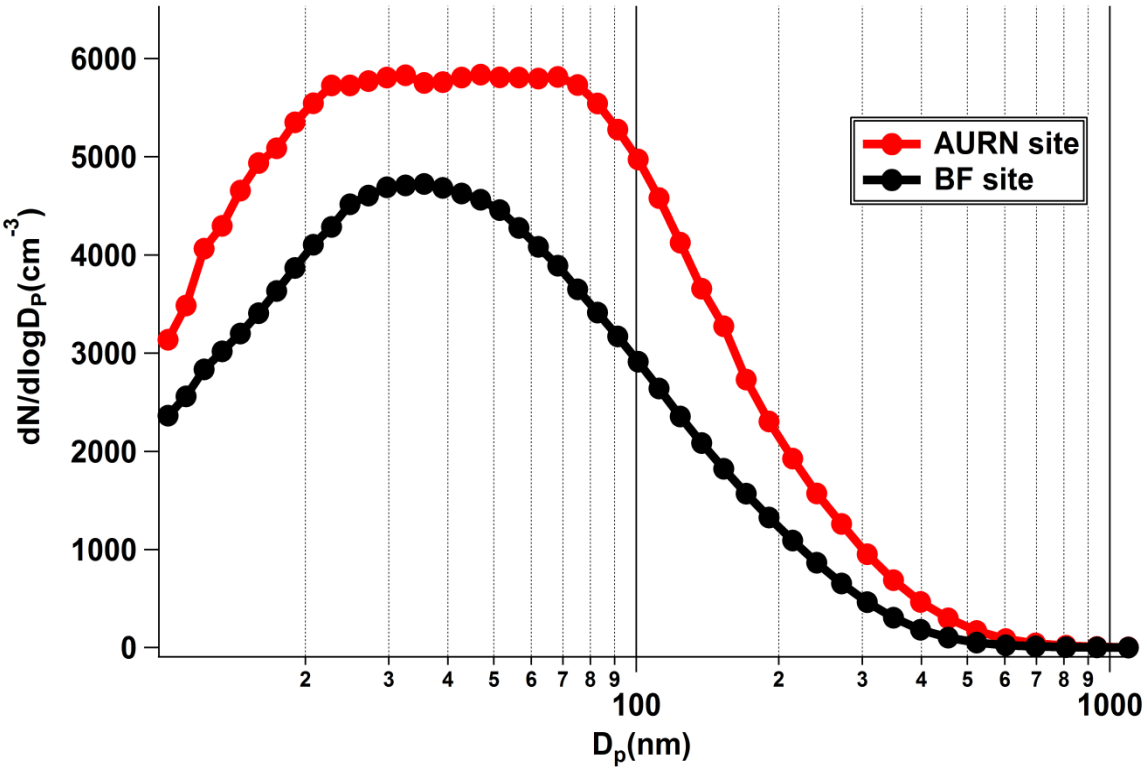

Figure 2: Particle number size distribution at AURN and BF sites.

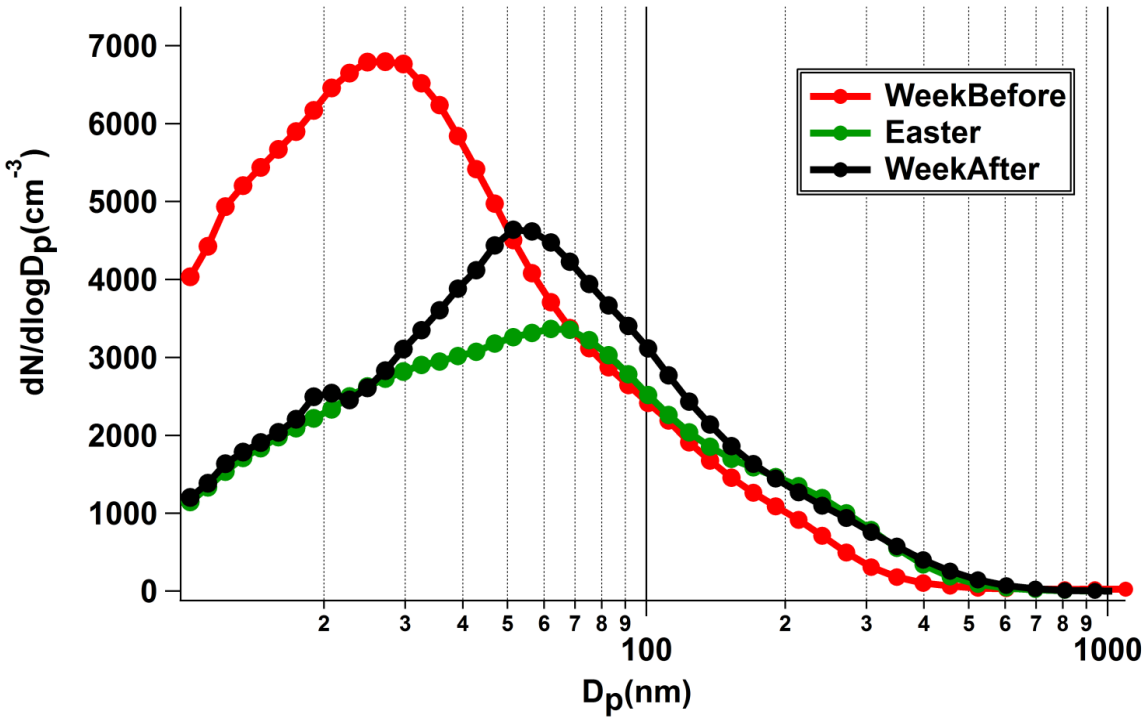

Figure 3: Particle number size distribution at Brookfield site. During week before Easter (Red line), Easter break (green line) and week after Easter (black line). Easter Holidays in Leicester: Mon 14th April – Fri 25th April 2014.

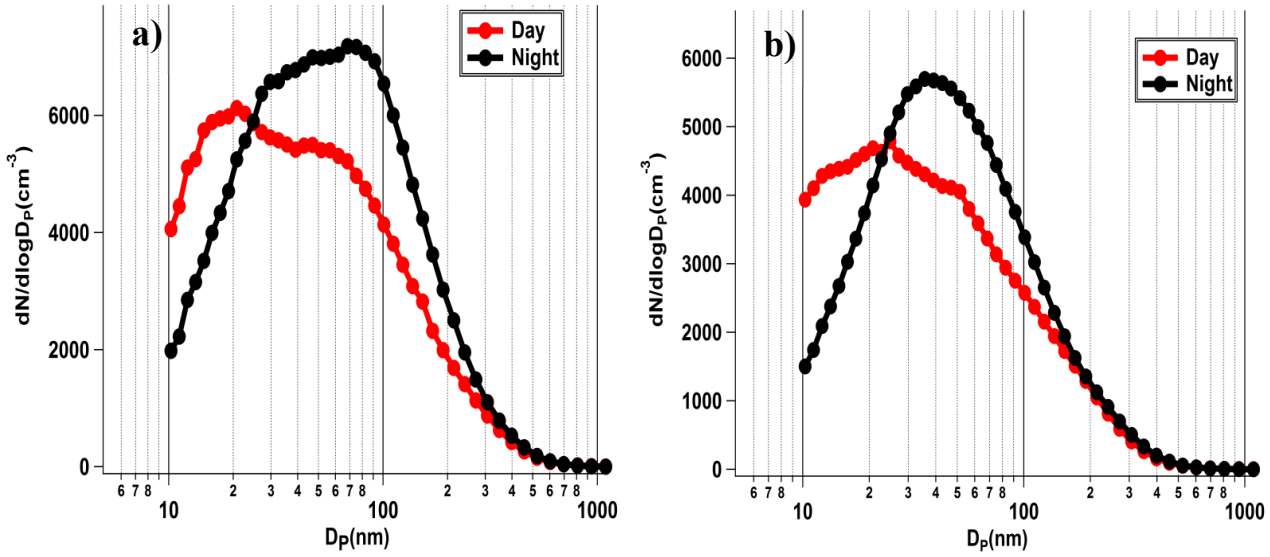

Figure 4: Particle number size distribution at a) AURN and b) BF sites under day time (7:00-19:00), and night (22:00-4:00) conditions.

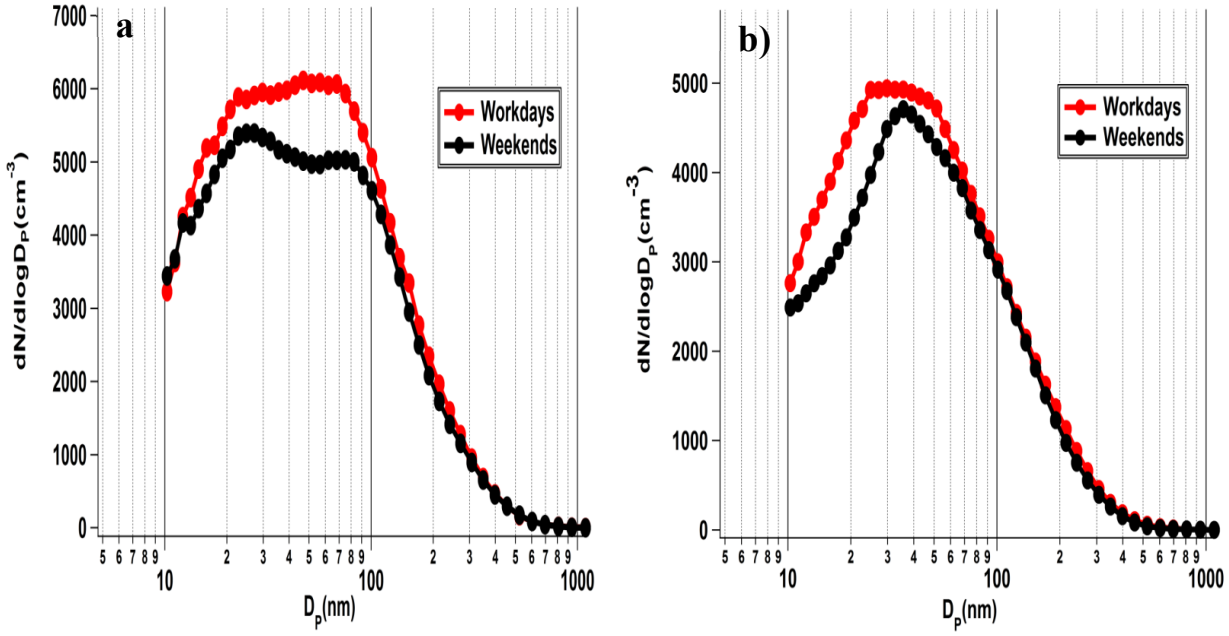

Figure 5: Particle number size distribution during weekends and weekdays at a) AURN and b) BF sites.

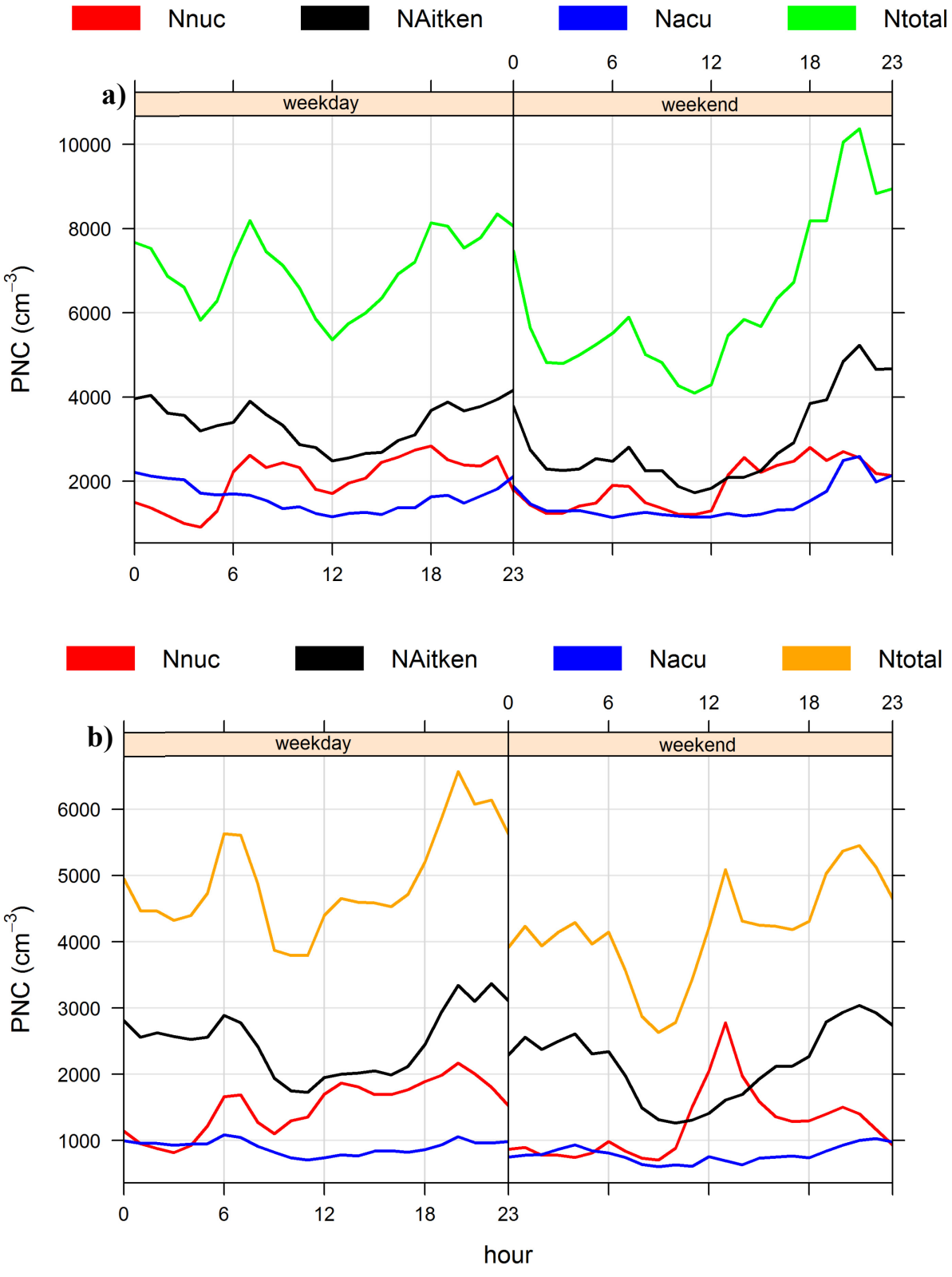

Figure 6: Mean diurnal variations of particle number concentration for a) AURN and b) BF sites. During workdays and weekends.

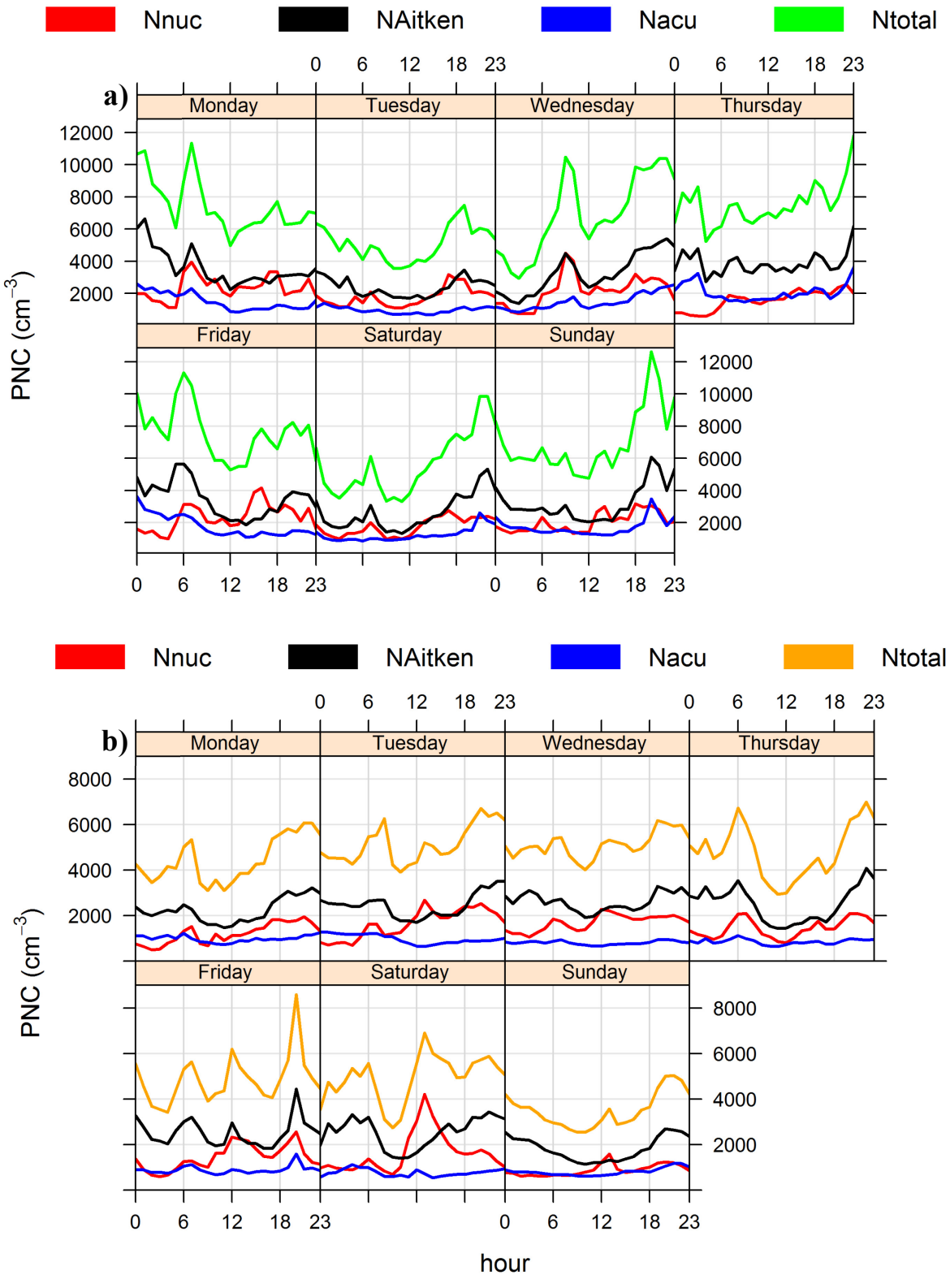

Figure 7: Weekly variation of particle number concentrations at a) AURN and b) BF sites.

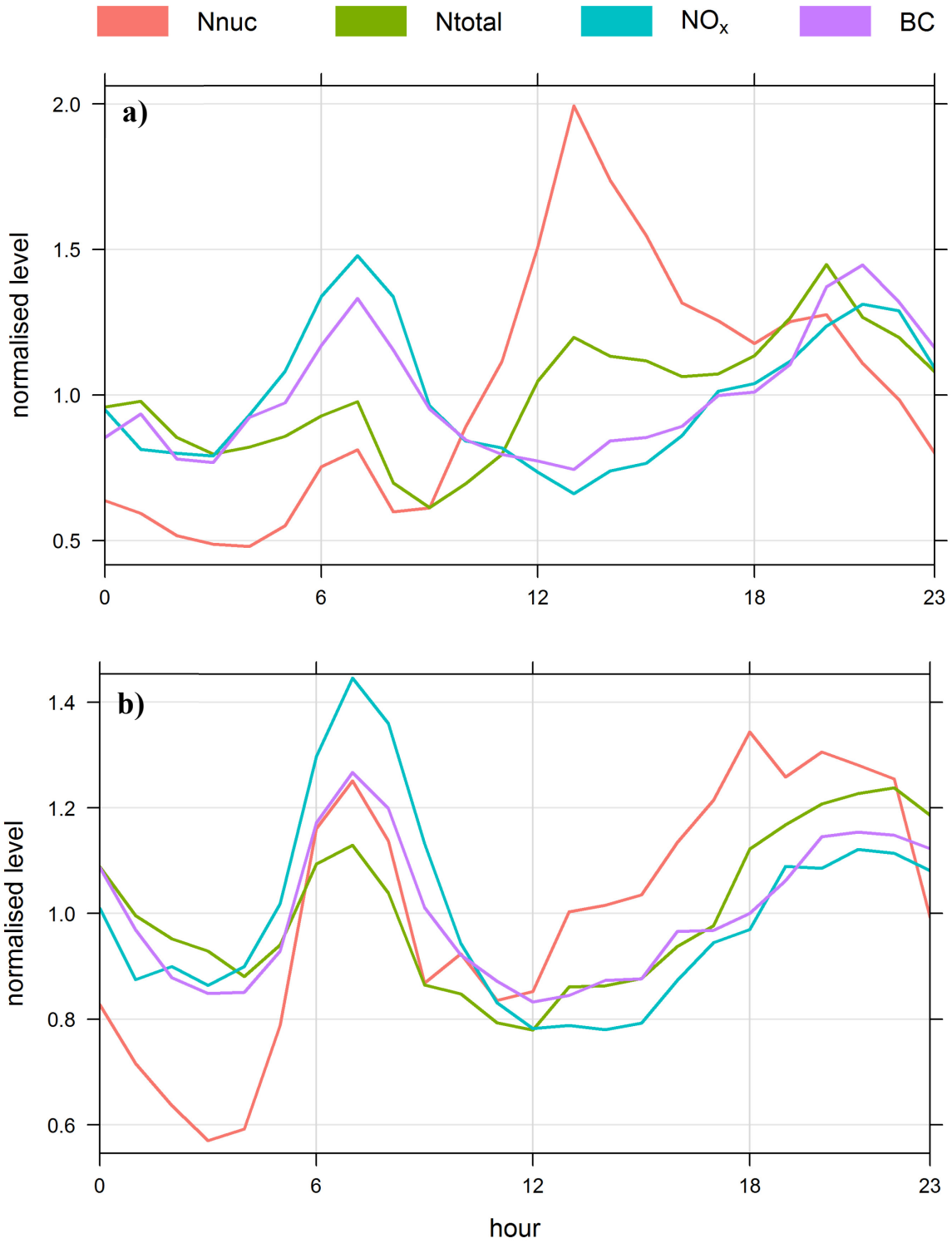

Figure 8: Diurnal variation of N_{nuc}, N_{total}, NO_X, and eBC for a) NPF event days (n=14), and b) Non-NPF event days (n=72).

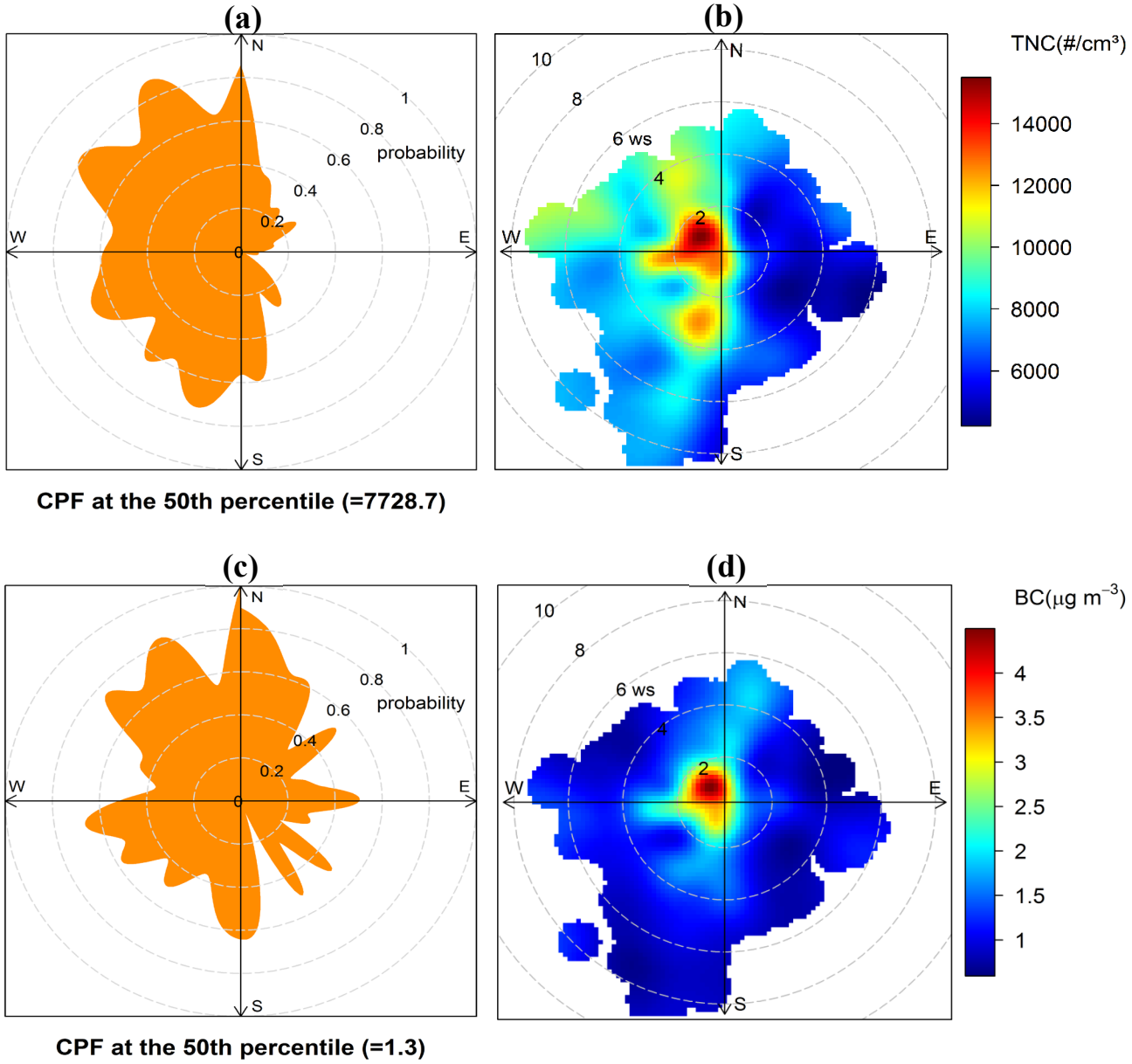

Figure 9: At AURN site a) CPF plot of TNC for concentrations >50th percentile (7728.7 # cm^{-3}), (b) Bivariate polar plot of TNC, (c) CPF plot of eBC for concentrations >50th percentile (1.3 µg m^{-3}), (d) Bivariate polar plot of eBC concentrations. The radial axis is wind speed in m s^{-1}.

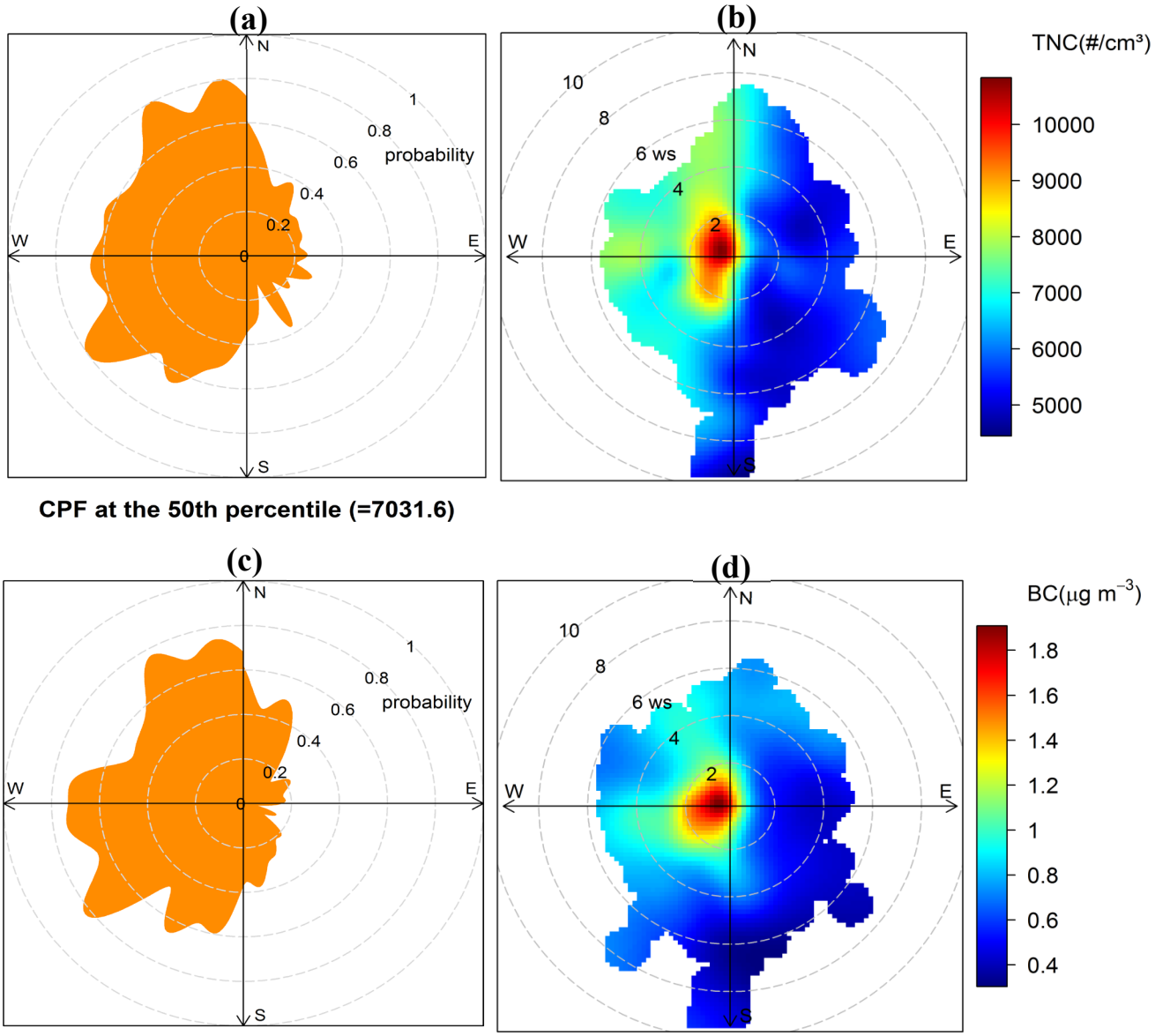

Figure 10: At BF site a) CPF plot of TNC for concentrations >50th percentile (7031.6 # cm^{-3}), (b) Bivariate polar plot of TNC, (c) CPF plot of eBC for concentrations >50th percentile (0.9 μg m^{-3}), (d) Bivariate polar plot of eBC concentrations. The radial axis is wind speed in m s^{-1}.

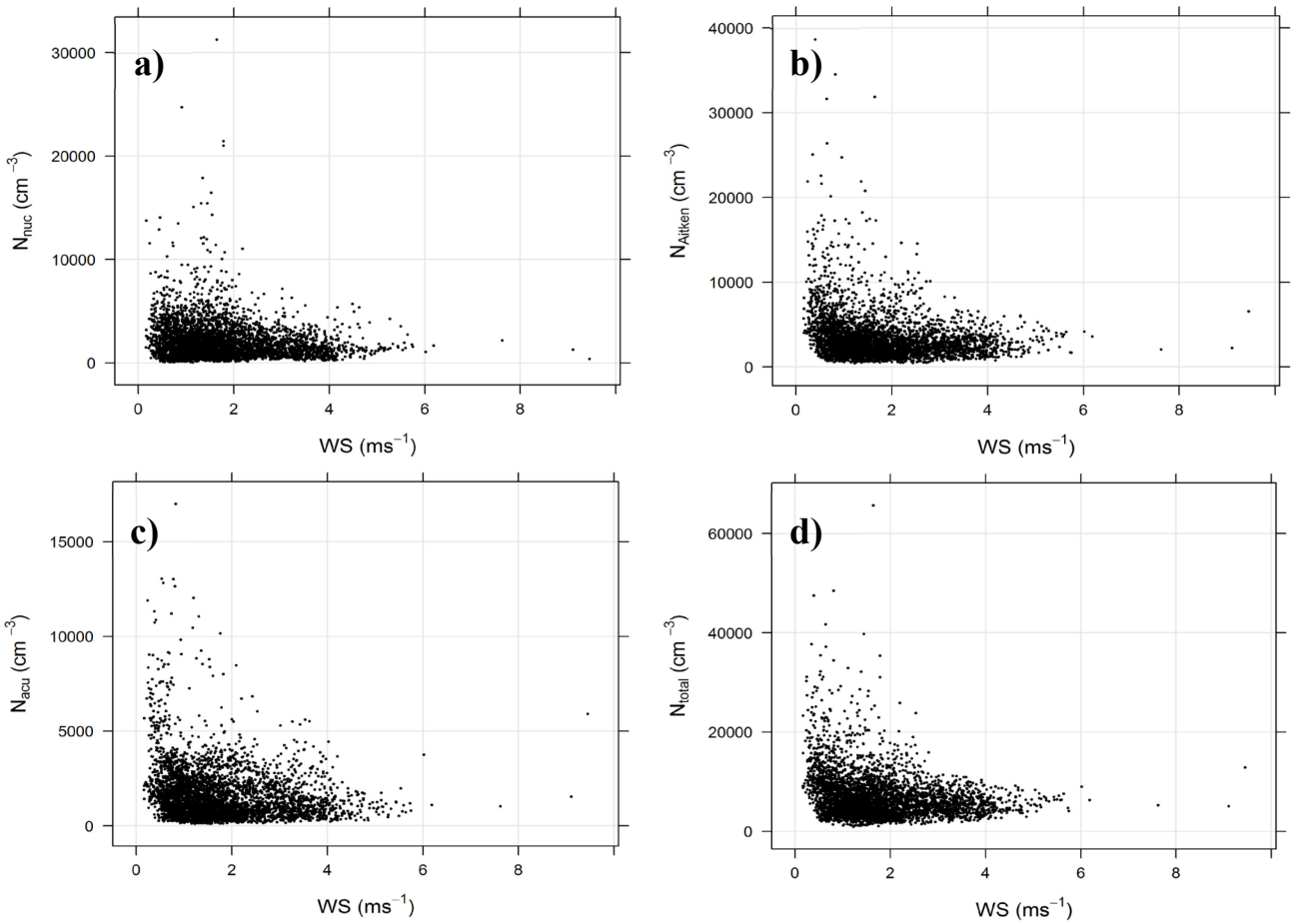

Figure 11: Correlation of the a) N_{nuc}, b) N_{Aitken}, c) N_{acu}, and d) N_{total} and wind speed for March 2014 at AURN site.

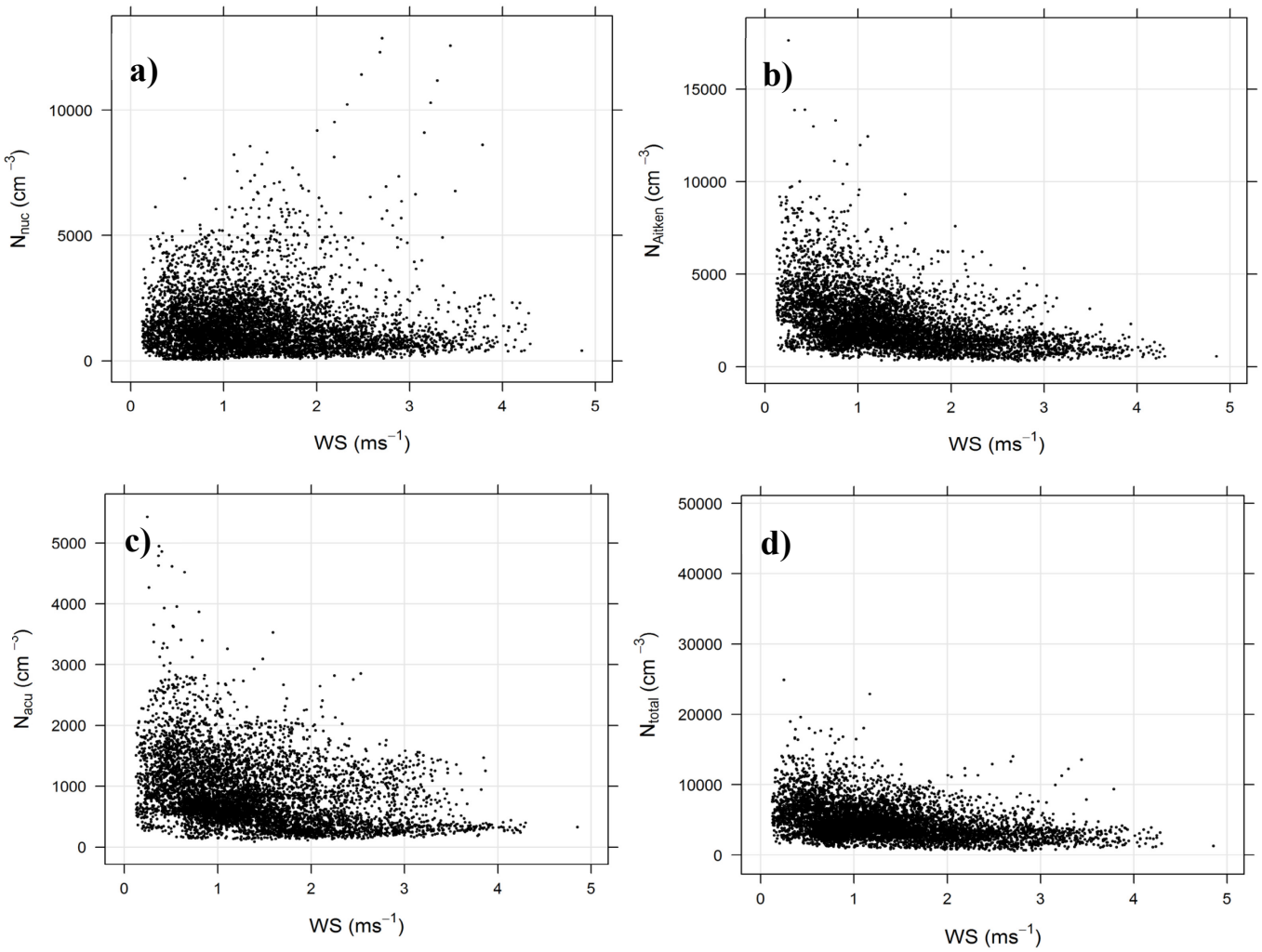

Figure 12: Correlation of the a) N_{nuc}, b) N_{Aitken}, c)N_{acu}, and d)N_{total} and wind speed for April and May 2014 at BF site.

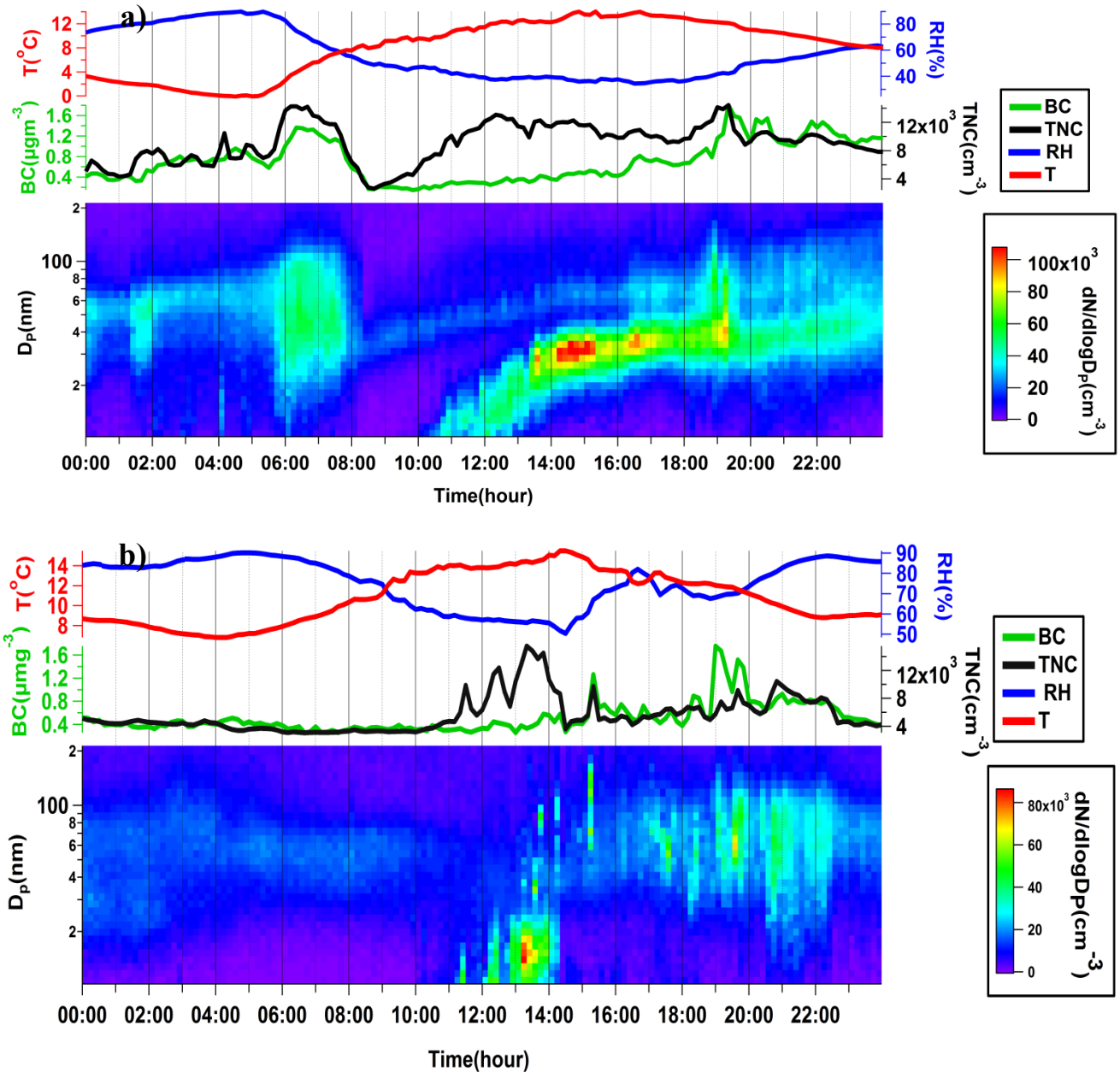

Figure 13: The NPF events measured on a) 3rd May 2014, and b) 27th April 2014. From bottom to top, the parameters are: (i) Average PNSD, (ii) N_{TOTAL}, and eBC mass concentrations, (iii) temperature, and relative humidity.